Fuel 331 (2023) 125856

Contents lists available at ScienceDirect

Fuel

journal homepage: www.elsevier.com/locate/fuel

Full Length Article

Modelling of carbonate rock wettability based on surface charge and calcite dissolution

Lawrence Opoku Boampong, Roozbeh Rafati *, Amin Sharifi Haddad

School of Engineering, University of Aberdeen, Aberdeen AB24 3UE, United Kingdom

ARTICLE INFO

Keywords:
Low salinity waterflooding
Zeta potential
Wettability alteration
Surface complexation model

ABSTRACT

The lack of consensus on the mechanisms underpinning low salinity waterflooding (LSWF) oil recovery has affected the successful implementation of LSWF in carbonate reservoirs. Many investigators link the improved oil recovery observed from LSWF to wettability alteration. Several models are proposed in the literature to study the wettability alteration mechanism. However, the reliability of some of the models is being contested, as they struggle to accurately predict the oil recovery trend. This study aims to develop a new wettability alteration model that can predict the performance of LSWF oil recovery processes. We propose a new wettability indicator (WI) that integrates three mechanisms (surface charge alteration/ζ-potential, calcite dissolution, and ion exchange) which, are suggested, dictate LSWF wettability alteration. The model was implemented in UTCHEM, which was coupled with PHREEQCRM, and was used to simulate several experimental LSWF oil recoveries.

The results produced from the simulations with the new model are consistent with experimental data. The outcomes from this study show that adsorption of crude oil is still possible even when the oil-brine and the rock-brine interfaces have the same polarities of ζ-potentials. The results further demonstrate that the improved oil recovery observed in LSWF is not always caused by the wettability alteration, but also caused by other factors such as rock quality and physical displacement. The outcome of the study also indicate that early injection of the low salinity brine can significantly improve the oil recovery.

Findings from this study can improve the understanding of the LSWF process. Moreover, the model proposed in this study can be applied in the design and planning of LSWF projects to estimate the performance of the LSWF.

1. Introduction

The interaction between the rock surface and oil in hydrocarbon reservoirs is controlled by the stability of the water-film between the oil and the rock surface [1]. A thick and stable water-film inhibits sorption of the oil active components onto the rock surface. It should be noted that stability of the water-film is dictated by the total disjoining pressure existing between the rock and the fluids. In other words, disjoining pressure can be described as the force that tends to separate the oil-brine and rock-brine interfaces, to maintain a stable water-film between the rock and the oil phase. Three forces, namely, van der Waals forces (VDWF), structural forces (SF) and double layer forces, contribute to the disjoining pressure, and the summation of these force components is expressed as the total disjoining pressure [2,3]. The structural forces are resulted from the ordered water molecules near the surface of the calcite mineral. The arrangement of the water molecules near the mineral's surface generates hydration forces, resulting in the formation of a thin water layer [4]. The double layer forces are electrostatic in nature and are induced by the development of charges at the oil-brine and rock-brine interfaces. van der Waals forces, on the other hand, describe the interactions between all molecules and atoms, including hydrocarbons [4]. For oil-brine-rock system, VDWF are always considered attractive while SF are repulsive. On the other hand, double layer forces can be attractive or repulsive depending on the polarities of ζ-potentials at the oil-brine and rock-brine interfaces. For instance, if the oil-brine and rock-brine interfaces have the same polarities, the double layer force will be repulsive. It is important to note that a positive disjoining pressure is always preferred to maintain a stable water-film between the oil and the rock. However, if the water film collapses, then, oil can easily adhere to the rock surface to change its wettability.

1.1. Mechanisms of crude oil adsorption

Buckley & Liu [5] categorised crude oil adsorption mechanisms into four groups: polar interactions, acid/base interactions, ion-binding, and

* Corresponding author.

https://doi.org/10.1016/j.fuel.2022.125856
Received 22 April 2022; Received in revised form 16 August 2022; Accepted 27 August 2022
Available online 12 September 2022

Nomenclature

Abbreviations

C1	capacitance between the 0-plane and the inner Helmholtz plane
C2	capacitance between the inner Helmholtz plane and the outer Helmoltz plane
F	Faraday constant
FW	formation water
FZI	flow zone indicator
HFU	hydraulic flow units
LSWF	low salinity waterflooding
MIE	multicomponent ion exchange
OHP	outer Helmholtz plane
pH_{IEP}	isoelectric point
R	universal gas constant
RQI	reservoir quality index
SCM	surface complexation model
SF	structural forces
SSA	specific surface area of calcite
SW	seawater
T	absolute temperature
TAN	total acid number
TBN	total base number
TLM	triple layer model
VDWF	van der Waals forces
WI	wettability indicator

Symbols

$[> C_{total}]$	total concentration of calcite surface species reacted with oil
dn_α	reacted moles of mineral α
f_α	volume fraction of mineral α
ΔG_{coul}	Coulombic interaction
i	reaction number
j	charge of the adsorbing oil species
K_{ro}	relative permeability to oil
K_{ro}^{hsw}	end-point relative permeability to oil at initial brine condition
K_{ro}^{lsw}	end-point relative permeability to oil at final state
K_{ro}^{o}	current end-point relative permeability to oil
K_{rw}	relative permeability to water
K_{rw}^{hsw}	end-point relative permeability to water at initial brine condition
K_{rw}^{lsw}	end-point relative permeability to water at final state
K_{rw}^{o}	current end-point relative permeability to water
K_t	permeability at current time step
K_{t-1}	permeability in previous time
M_α	molar mass of mineral α
$M_{calcite}$	molecular weight
n_α^0	initial amount of mineral α present
n_α^t	number of moles of mineral α at current time
$n_{calcite}$	amount of calcite in mol
n_α^{t-1}	number of moles of mineral α in previous time
S_w	water saturation
S_{wc}	connate water saturation
V_b	grid block bulk volume
V_{H_2O}	volume of solution
$V_{m\alpha}$	molar volume of mineral α
Δz_{bk}	charge change in the bulk solution
Δz_m	charge change at the mineral surface
$\Delta z_{2,ob}$	charge change at the oil-brine outer Helmholtz plane
$\Delta z_{2,rb}$	charge change at the rock-brine outer Helmholtz plane

Greek letters

α	mineral type present in the carbonate rock
β_i	wettability indicator calculated for reaction i
$\beta_i^{initial}$	initial wettability indicator calculated for reaction i
β_i^{final}	final wettability indicator calculated for reaction i
β_i^t	wettability indicator for reaction i calculated at current time
β_{total}^{int}	total relative permeability interpolant
σ	calcite surface species type
ρ_α	mineral density
φ_e	porosity
φ_z	normalised porosity index
φ_t	porosity at current time step
φ_{t-1}	porosity in previous time step
ψ_{OHP}	potential at the outer Helmholtz plane
ψ_{rb}	potential at the rock-brine outer Helmholtz plane
ψ_{ob}	potential at the rock-brine outer Helmholtz plane
ω_σ	weight factor of calcite surface species σ involved in the oil adsorption reaction
ζ-potential	zeta potential

Subscripts/Superscripts

hsw	high salinity water
lsw	low salinity water
i	reaction number
ob	oil-brine
o	oil
rb	rock-brine
t	time step
w	water

surface precipitation. Acid/base interactions denote the condition whereby the polar functional groups of both the mineral and the oil act as acids and bases (by losing or gaining protons) and become charged. For instance, the carboxylic component of crude oil can dissociate at high pH condition and become negatively charged. Similarly, a carbonate mineral can adsorb hydrogen ions to its surface and become positively charged. The attractive electrostatic or columbic forces generated can collapse the water-film (i.e., negative disjoining pressure), and the oil components can be adsorbed at the mineral surface [5] to change its wettability (reaction A). It is worth mentioning that the attraction between the mineral surface and the oil component involves opposite charges. Ion-binding interactions occur in the presence of multivalent ions (e.g., Ca^{+2}, Mg^{+2}) such that the acidic/basic crude oil-mineral surface charged groups are linked to each other by these ions (reaction B). It should be noted that the same multivalent ion binds the mineral surface group to the oil surface species [6]. Polar interactions, on the other hand, happen in the absence of water between the rock and the crude oil, where the oil directly sorbs onto the mineral surface. Surface precipitation occurs when the crude oil contains significant amount of asphaltenes. The asphaltenes can precipitate from the oil and react with the carbonate rock to alter its wettability. The mineral can become more oil-wet when the oil is a poorer solvent to the asphaltenes [7].

$$>CaOH_2^+ + COO^- <=> >CaOH_2\ldots COO \quad (A)$$

$$>CO_3^- + Ca^{+2} + COO^- <=> >CO_3Ca\ldots CO\ O \quad (B)$$

Brady et al. [8] further classified the adsorption mechanisms into

two main groups as directly sorbed oil and indirectly sorbed oil. While directly sorbed oil involves the adsorption of the crude oil directly to the mineral surface (e.g., polar interactions), indirectly sorbed reactions involve three-layer oil/water/rock configuration (e.g., acid/base & ion-binding interactions). They indicated that the indirectly sorbed oil is loosely held, and that the sorption reaction is reversible. However, the directly sorbed oil is retained on the mineral surface and can only be removed by heroic methods such as surfactant flooding, CO_2 injection and steaming.

It is important to note that the degree of crude oil adsorption is very much dependent on several factors including oil composition, formation water composition and/or salinity, pH, temperature and rock mineralogy [6,9–11]. Carbonate mineralogy can influence the initial wetting condition of the reservoir and any subsequent change in the wettability. Carbonate rock composed of only calcite, or only dolomite, or a mixture of different minerals, can react and behave differently under the same conditions. Mahani et al. [12] studied the relation between carbonate mineralogy and wettability by measuring the contact angle. Their results showed different contact angle value for the two carbonate patches (limestone and dolomite) under the same conditions. For instance, in formation water (FW), the obtained contact angle for the limestone was around 98° whereas the dolomite rock measured a contact angle of about 68°. In switching the brine to seawater (SW), the measured contact angle for the limestone was about 92° and that for the dolomite rock was about 65°. Mahani and co-workers concluded, that under the same conditions, a dolomite surface has a smaller contact angle than a limestone surface. However, the smaller change in the dolomite initial contact angle, compared with the limestone, was attributed to the stronger adhesion forces between the dolomite mineral and the adsorbed oil. Su et al. [13] also investigated the effects of carbonate mineralogy on wettability through the contact angle measurement. They observed that under the same conditions, the carbonate rock composed of large amount of dolomite showed smaller contact angle values than the one composed of large amount of calcite. However, similar to the results of Mahani et al. [12], they indicated that the maximum change in the contact angle is fairly linear with the calcite content of the rock, implying that carbonate mineralogy can affect the wettability.

The initial wettability of carbonate rocks is mainly influenced by the polar organic components present in crude oil [11]. The polar organic components in crude oil control the interaction, and consequently, affect reactions with the carbonate rock surface. Polar organic components present in crude oil are usually classified into acidic and basic components, where the acidic components are primarily carboxylic acids. The basic components, on the other hand, are present as nitrogen-based aromatic molecules [11]. It is worth noting that the acidic and the basic oil components are quantitatively determined by the total acid number (TAN) and the total base number (TBN), respectively. That is, for example, a high TAN corresponds to the oil containing large amount of the acidic components. It has been proposed that the ratio of the TAN to the TBN significantly affects the initial wetting condition, and that TAN is a critical parameter which mostly dictates the wetting state of the carbonate rock. Thus, increasing TAN tends to produce an oil-wet carbonate reservoir [14].

Another important parameter that affects the initial wetting state of carbonate rocks is the composition, salinity, and pH of the formation water. At high pH, dissociation of the carboxylic acid is increased, producing negative charges at the oil-brine interface. The isoelectric point (pH_{IEP}) for different oils were found to occur at pH below 5[1], suggesting that most crude oils will exhibit negative ζ-potential at high pH values. Calcite, however, has pH_{IEP} near pH of 8.2[8], hence, below this value the calcite surface will generate positive ζ-potential. It should be noted that pH of most carbonate reservoirs is between 7 and 8[15], therefore, the initial wettability of most carbonate reservoirs is oil-wet or mixed-wet. This is because the calcite surface which is more likely to be positive will have strong affinity to the negatively charged oil species at the reservoir pH. Composition of the formation water, particularly, availability of multivalent ions (eg: Ca^{+2}, Mg^{+2}, CO_3^{-2}, SO_4^{-2}) can significantly impact the initial wettability of the carbonate rock. Zaheri et al. [16] observed that increasing the Ca^{+2} ion content in the formation water increased the oil-wetness of the carbonate rock (i.e., the initial wettability becomes more oil-wet) as they measured large contact angle values when Ca^{+2} ion concentration in the formation water is increased. Zaheri et al. [16] explained that increasing the Ca^{+2} ion concentration in the formation water increased the positive charge density on the carbonate rock surface. Therefore, the carboxylic acids in the crude oil due to their negative charges are more attracted to the carbonate surface, rendering it oil-wet.

Temperature is also a vital parameter that affects initial wettability and any change in the subsequent wetting of carbonate rocks. Temperature impacts the oil/brine and rock/brine interface interactions, and increasing the aging temperature of carbonate rock significantly increases the oil wetness of the carbonate rock [17].

1.2. Mechanisms of LSWF and crude oil desorption

Initially, any reservoir is in equilibrium with its fluids. The injection of brine, whose composition and/or salinity is different from the initial reservoir brine, into the reservoir disturbs the reservoir equilibrium. This induces rock-oil–water interactions which can result in the release of the adsorbed oil from the rock surface. LSWF was observed in 1959 when Martin [18] identified higher oil production from freshwater injection in sandstone. However, it was not recognized until Morrow et al. [19–22] began deeper investigation. Despite the numerous reported cases of positive impact of LSWF on oil recovery [15,19,21,23–28], the mechanisms behind the improved oil recovery remain poorly understood.

Many studies conducted so far associate the improved oil recovery to wettability alteration, however, the underlying mechanism behind the wettability alteration is not certain. Multicomponent ion exchange (MIE) has been proposed as the main mechanism responsible for the LSWF incremental oil recovery [29]. MIE involves the exchange of ions between the aqueous phase and the mineral surface, and this interaction can result in the liberation of oil from the rock surface. It is suggested that adsorption of some specific ions (Ca^{+2}, Mg^{+2}, SO_4^{-2}) can significantly impact the oil desorption, shifting the reservoir from its initial wetting condition to a more water-wet state [23–26,30]. Zhang et al. [23,31] explained that, during the injection of low salinity water into a carbonate reservoir, SO_4^{2-} is adsorbed onto the mineral surface, which will co-adsorb Ca^{2+} and Mg^{2+} (due to decrease in electrostatic repulsion induced by the SO_4^{2-}). The adsorbed Ca^{2+} and Mg^{2+} will react with the adsorbed carboxylic groups, releasing them from the mineral surface. Therefore, SO_4^{2-} acts as catalyst during the MIE reactions. However, Gupta et al. [32] reported incremental oil recovery of 9 % OOIP from the injection of a low salinity water which is devoid of SO_4^{-2} ion. Other investigators [33,34] have also not observed any additional oil recovery or change in the contact angle by increasing the SO_4^{-2} ion concentration or varying the Ca^{+2}/Mg^{+2} ratio in the injection brines.

It is envisaged that mineral dissolution can also increase oil recovery as a result of low salinity waterflooding. Injecting a brine which contains low Ca^{+2} concentration can result in the dissolution of calcite mineral, and if the dissolution occurs at a location where oil is adsorbed, the oil can be released from the rock surface. This can shift the reservoir to a more water-wet condition [9,35]. Other researchers support dissolution as one of the LSWF mechanisms [26,36–41]. On the contrary, Nasralla et al. [42] established that calcite dissolution cannot be the main mechanism of LSWF in carbonate reservoirs. They reported that brines, that could not dissolve calcite, recovered more oil, whereas brines that dissolved calcite did not produce additional oil. It is proposed that dissolution may only enhance the LSWF as a secondary mechanism, and this is only relevant at a laboratory scale [12].

We have earlier indicated that water film stability is subject to the electrical charges that are generated at the oil-brine and the rock-brine

interfaces [4,43–45], and this implies that wettability is related to the surface charges. Sari et al. [45] observed a strongly water-wet condition from the contact angle experiment they conducted. They reported that the measured contact angle values were consistent with the measured ζ-potential values. Sari et al. [45] mentioned that a repulsive double layer force exists in the porous rock as they measured the same polarities of ζ-potentials at the oil-brine and rock-brine interfaces. Their observations are consistent with the outcomes reported by Mahani et al. [12]. This suggests that brine, which can generate same polarities of ζ-potentials at the oil-brine and rock-brine interface, will produce a more stable water film between the oil and the rock surface, making the reservoir more water-wet [46]. In contrast, Hiorth et al. [9,10] concluded that surface charge is not the main mechanism controlling the wettability alteration and the oil recovery. They indicated that, whereas the oil recovery increased during the entire observed temperature range, the surface potential remained almost constant. Hiorth et al. [9,10] proposed that the relationship between oil recovery and temperature cannot be captured by the surface potential.

Other mechanism suggested to govern LSWF is the increase in pH during low salinity water injection [47]. Exchange of ions occurring at the mineral surface, as well as dissolution of the carbonate rock, can raise the pH [41,47]. The high pH-brine can react with the acidic oil component and generate in-situ surfactant. The interfacial tension (IFT) between oil and water can be reduced by this surfactant, and oil recovery increased. Therefore, LSWF behaves in a similar way to alkaline flooding; the elevated pH generates a more water-wet condition [47]. Nonetheless, other researchers have disputed this hypothesis. They claim that generation of in-situ surfactant is unrealistic, considering the degree of pH increment observed from the LSWF [29,41]. Lager et al. [29] pointed out that the CO_2 gas existing in most reservoirs will act as a buffer and an increase in pH to a higher value is unlikely to occur. Furthermore, other investigators did not observe a correlation between oil recovery and IFT [31].

The above discussions demonstrate that the wettability alteration mechanisms are not consistent, and that the lack of consensus on the mechanisms underpinning LSWF has impacted the successful implementation of LSWF in carbonate reservoirs [48,49].

1.3. Wettability alteration models for LSWF

Attempts have been made by various investigators to further probe and understand the relationship between oil recovery and wettability alteration using numerical models. It is worth noting that, in the modelling of LSWF oil recovery, the wettability alteration effect is studied via a shift in the relative permeability curves. Two sets of relative permeability curves are employed; one for the initial conditions, formation water, and the other for the final state, where the concentrations and components in the aqueous phase in the pore-spaces are the same as the injected low salinity water. A wettability alteration parameter (generally referred to as wettability indicator or wettability interpolant) is then applied to interpolate between the two relative permeability curves. This produces a relative permeability consistent with the current carbonate-oil-brine condition. Therefore, the wettability alteration is measured by the correlation between the oil recovery and the wettability indicator. In other words, the wettability indicator (a mathematical expression) denotes the mechanism(s) proposed to cause the wettability alteration.

Several wettability indicators have been proposed in the literature, and the theorical basis (i.e, mechanisms) for the development of these models differ from one another. Some of the proposed models are based on the salinity of the brine [50], dissolution of the reservoir rock [9,10,35,51,52], and the concentration of adsorbed specific ion on the rock surface [41,53,54]. Others have used the amount of rock and oil surface species [8,55,56], concentration of adsorbed carboxylic oil component [6,57,58], ionic strength [59], concentration of aqueous ion [60], and migrated fines [61]. Some works have also applied the Deryaguin–Landau–Verwey–Overbeek theory (DLVO theory) to study the wettability alteration mechanism [62–65]. It should be noted that some of the WI models failed to predict the oil recovery trend accurately when used for LSWF simulations, therefore, their reliability is being contested in the literature.

The salinity dependent WI model was suggested by Jerauld et al. [50]. This model assumes that the wettability alteration is linearly dependent on the salinity of the brine. Therefore, the salinities of high salinity water and low salinity water are used as the threshold, between which the interpolation is carried out. Although some investigators have observed a linear relationship between oil recovery and the salinity of the injection brine [15,27,66], others have reported results where no correlation exists between oil recovery and the salinity of the injection brines [25,67,68]. It is worth mentioning that the wettability alteration is not exclusively caused by the salinity of the brine, but rather, it is related to the geochemical reactions that take place inside the reservoir (as the brine is injected). These reactions are influenced by several parameters of which salinity is one. Therefore, using salinity of the brine as a WI may not predict accurately the LSWF oil recovery.

Hiorth et al. [9,10] proposed calcite dissolution as the dominant mechanism controlling wettability alteration; however, they did not develop WI to model this mechanism. Later works by Evje & Hiorth [35], Korrani et al. [51], and Kleppe & Khalediadusti [52] suggested a WI based on the calcite dissolution. The model assumes that dissolution of calcite liberates oil from the rock surface, shifting the wettability towards a more water-wet condition. Therefore, the developed WI is linked to the amount of the dissolved calcite mineral. However, Evje & Hiorth [35] and Kleppe & Khalediadusti [52] did not validate their model against any experimental data. Moreover, Korrani et al. [51] reported that excluding surface reactions from the model resulted in no improved oil recovery when this WI was applied to a field scale.

Some researchers [41,53,54] also associated the wettability alteration to the equivalent fraction of specific ion adsorbed at the rock surface. The equivalent fraction corresponds to the exchangeable amount of the selected ion [53], which can be Ca^{+2}, Mg^{+2}, or Na^{+} ions, obtained at the mineral surface. Therefore, an increase in the equivalent fraction of the selected ion shifts the reservoir towards a more water-wet condition [41,53,54]. This WI was formulated based on the ion exchange mechanism proposed by Lager et al. [29]. Hence, the WI was developed using the ion exchange model. In ion exchange models, the rock is considered as an exchanger, where the ionic species on the exchanger can be displaced by other ions in the aqueous phase. It should be noted that sorption of metal ion is greatly dependent on the electric charge (electric potential) of the surface [69], however, the electric charge effect is not considered in ion exchange models. Furthermore, much information related to the calcite-brine interface interactions is not included in ion exchange models [70]. The ion exchange model does not consider the interactions of the oil phase with the brine and/or the rock. Therefore, predicting the wettability alteration and oil recovery with this model may not be accurate.

Qiao et al. [6,57] introduced the concept of using the concentration of adsorbed carboxylic oil species (i.e., the number of carboxylates bonds) to model the LSWF. The wettability alteration was linked to the number of carboxylates bonds found on the rock surface. Therefore, the reservoir becomes more water-wet as the concentration of adsorbed carboxylic oil component minimises. However, the proposed model lacks consistency and has more adjustable parameters [71]. In some cases, electrical double layer was used while non-electrical double layer was considered for other cases, although the simulated experimental data were conducted under similar conditions [71]. Furthermore, the Gouy-Chapman equation used by the authors to relate surface charge to surface potential is only valid for systems comprising of monovalent ions [71], however, the simulated data contained divalent ions. Moreover, Qiao et al. [6,57] did not include the basic oil interactions in their developed model.

Korrani & Jerauld [72] also suggested stability number as a

wettability indicator to model LSWF. Stability number, calculated from the ratio of electrostatic force to van der Waals force, requires both the oil-brine and the rock brine interface ζ-potentials. However, the Gouy-Chapman relation used by Korrani & Jerauld [72] in estimating the ζ-potentials is valid for only symmetrical solutions [71]. Moreover, the limiting values of the stability number were given as 0.1 and 2[59], indicating that polarities of the oil-brine and the rock brine interface ζ-potentials are always the same. However, the ζ-potentials can have different polarities, resulting in negative stability numbers. This was highlighted by Bonto et al. [71,73] as they calculated negative values for the stability number, which nullifies Korrani & Jerauld(90) limiting values. This proposed model could not also predict the experimental oil recovery trend [71,73]. Korrani et al. [59], in another work, proposed that the wettability is controlled solely by the ionic strength. The authors assumed that the dominant mechanism controlling the wettability alteration is the expansion of the electrical double, which is related to the ionic strength. Therefore, the reservoir shifts to a more water-wet condition as the ionic strength decreases. It should be noted that the carbonate-oil-brine interactions that control wettability are more complicated, therefore, describing the LSWF by a single parameter like ionic strength, cannot capture the complexities of the wettability-related reactions. Consequently, the oil recovery did not show good correlation to this WI when the WI was used to simulate LSWF data [71].

Bond product sum, proposed by Brady et al. [8,55], denotes the sum product of oppositely charged oil-brine and rock-brine surface species. The wettability alteration is linked to the value of the bond product sum, such that, the reservoir is classified as oil-wet when the calculated bond product sum is higher, otherwise, the reservoir is water-wet. However, no correlation was found between bond product sum and the oil recovery [73]. Recently, Bonto et al. [71,73] proposed wettability indicator involving ζ-potentials and surface species; however, it was developed purposefully for chalk reservoirs. Moreover, Bonto et al. [71,73] in formulating their WI, assumed that only the acid-base interactions control the wettability. Furthermore, they also did not consider the oil-brine charge effect in their WI calculation.

Variations in the studies found in the literature indicate that the main mechanisms causing the wettability alteration and the improved oil recovery are still not certain. Therefore, the mechanisms of LSWF (wettability alteration) remain a significant research area in the hydrocarbon development field [74].

This study aims at developing a new wettability indicator that can handle the complexities of the carbonate-oil-brine interactions. We proposed a new WI that incorporates almost all the mechanisms (i.e., surface charge alteration/ζ-potential, calcite dissolution, and ion exchange mechanisms) suggested to be dictating the LSWF wettability alteration. Scope of the study includes the following: (i) development of a new wettability indicator and validating it with core flooding results, (ii) identifying the optimum brine salinity for low salinity projects, and (iii) using the developed model to study the effects of injection rates and timing of the low salinity injection on oil recovery. Results of the study can improve our existing knowledge and understanding of the fundamentals of the LSWF process. The model proposed in this study can also be used as a tool in the designing and planning of LSWF projects to give a forecast of the oil recovery when the LSWF is implemented. It should be noted that the current study is an extension of our previous work where the WI was developed from only the ζ-potentials [75].

2. Methodology

In this study, UTCHEM was coupled with PHREEQCRM, which was used to simulate LSWF process. UTCHEM is a three-dimensional, non-isothermal, multiphase flow reservoir simulator developed by the University of Texas at Austin [76]. It is used to simulate many enhanced oil recovery processes. PHREEQC [77,78], on the other hand, is a general-purpose geochemical simulator, which is capable of modelling interactions between water and gases, surface complexes, minerals, ion exchangers, and solid solutions. However, coupling PHREEQC with multiphase simulators can be inefficient when running millions of calculations. Therefore, PHREEQCRM [78]‘ is designed specifically to ease coupling of PHREEQC with multiphase flow simulators. It offers a high-level interface that permits flow simulators to implement geochemical reactions with a minimum amount of programming, whilst ensuring utilisation of the full functionality of PHREEQC’s reaction capabilities. Thus, it allows one to use PHREEQC as a reaction engine for the transport simulator. This section describes the method that was used to simulate the LSWF oil recovery process using the coupled UTCHEM-PHREEQCRM simulator. Description of the simulated geochemical reactions, calculated with a surface complexation model (SCM) is provided first. We then described the method used to couple PHREEQCRM with UTCHEM. Finally, description of our wettability alteration modelling approach is presented.

2.1. SCM for the carbonate-brine and oil-brine interface interactions

The study uses a triple layer model (TLM) developed in a previous work [75] for the calculation of the carbonate-brine-oil interactions. For the oil-brine interface reactions, the model considers two active sites, namely, acid site and base site. The site-densities (i.e., acid site-density, NCOOH and base site-density, NH) are calculated from the TAN and the TBN of the oil, respectively, using Equation (1) – (2)[72,79]:

$$N_{COOH}\left(\frac{no.sites}{nm^2}\right) = 0.602 \times 10^6 \times \frac{TAN(\text{mg KOH/g oil})}{1000 \times a_{oil\times MW_{KOH}}} \quad (1)$$

$$N_{NH}\left(\frac{no.sites}{nm^2}\right) = 0.602 \times 10^6 \times \frac{TBN(\text{mg KOH/g oil})}{1000 \times a_{oil\times MW_{KOH}}} \quad (2)$$

where: a_{oil} denotes oil specific surface area in m^2/g, and MW_{KOH} is molecular weight of KOH. The TAN and TBN, therefore, are input parameters for the acidic and the basic sites-densities determination. Two calcite lattice ions, calcium (>Ca) and carbonate ($>CO_3$) were considered, and based on Stipp [80], fractional charge of 0.25 was assumed for calcite surface (i.e., $>Ca^{+0.25}$, $>CO_3^{-0.25}$). We assumed site-density of $4.95/nm^2$ for each of the calcite lattice ions, consistent with literature [75,81,82]. Specific surface area of oil and calcite was set to 1 m^2/g based on Korrani & Jerauld [72], Brady et al. [55], and Bonto et al. [71]. Protonation/deprotonation reactions were modelled at the 0-plane while other sorption reactions were modelled at the inner and outer Helmholtz planes. It should be noted that two capacitance values are required in TLM: C1 (capacitance between the 0-plane and the inner Helmholtz plane) and *C*2 (capacitance between the inner Helmholtz plane and the outer Helmholtz plane), and following other investigators [70,71,83,84], we used C1 = $2.8 F/m^2$ and *C*2 = $4.5 F/m^2$. The detailed description of the TLM can be found elsewhere [75].

We calculated ζ-potential from the model assuming that slip plane coincides with the outer Helmholtz plane (OHP)[70,71,83,85,86]. That is, ζ-potential = ψ_{OHP}, where ψ_{OHP} is the potential at the OHP calculated

Table 1
Oil-brine interface reaction parameters [75]. Z0 and Z1 are change in charge at the 0-plane and the inner Helmholtz plane (IHP), respectively.

No.	Oil-Brine Surface Reactions	log_K at:25 °C	50 °C	Z0	Z1	ΔH°, kJ/mol
1	>RCOOH ⇔ > $RCOO^-$ + H^+	−4.8	−4.5	−1	0	22.13
2	>N + H^+ ⇔ >NH^+	3.92	3.5	1	0	−30.99
3	>RCOOH + Na^+ ⇔ >RCOONa + H^+	−4.2	−4.52	−1	1	−23.61
4	>RCOOH + Ca^{+2} ⇔ > $RCOOCa^+$ + H^+	−3.1	−3.63	−1	2	28.04
5	>RCOOH + Mg^{+2}⇔ > $RCOOMg^+$ + H^+	−3.58	−3.2	−1	2	−39.1
6	C1, F/m^2	2.8				
7	*C*2, F/m^2	4.5				

by PHREEQC. The optimized reaction parameters are shown in Table 1 and Table 2.

Carbonate mineral dissolution/precipitation reactions were also considered in the model. It is essential to note that in PHRREQCRM, the initial amount of mineral α present in the carbonate rock, n_α^0, is defined in unit of mol per unit volume of water in the grid block. The n_α^0 is then calculated as:

$$n_\alpha^0 = \frac{\rho_\alpha(1-\varphi)f_\alpha}{M_\alpha \varnothing S_w} \tag{3}$$

where ρ_α denotes mineral density $\left(\frac{\text{kg}}{\text{L}}\right)$, M_α is molar mass of mineral α $\left(\frac{\text{kg}}{\text{mol}}\right)$, f_α is volume fraction of mineral α, φ is porosity, and S_w denotes water saturation. Derivation of Equation (3) is provided in Appendix A. PHREEQCRM, after reading the input file, automatically converts the mineral amount from $\frac{\text{mol}}{\text{L of } V_{H_2O}}$ to mol, where V_{H_2O} denotes volume of solution.

2.2. Coupling UTCHEM with PHREEQCRM

Transport and geochemical reactions occur simultaneously in fluid flow, however, this work solved transport and reaction equations separately, using UTCHEM for fluid transport and PHREEQCRM for.

geochemical reaction calculations. Coupling of UTCHEM and PHREEQCRM was achieved using the sequential non-iterative coupling approach reported by Parkhurst & Wissmeier [78], Korrani et al. [87–89], and Boampong et al. [75]. In this method, iteration between the two simulators is not required [89]. Thus, chemical reactions are not involved when UTCHEM solves the mass conservation equation. Below is the summary of steps followed to couple UTCHEM and PHREEQCRM (the detailed procedure is provided in Boampong et al. [75]):

1. UTCHEM calculates elements concentration (mol/l) in brine after each time-step in each numerical grid-block.
2. These data are exported to PHREEQCRM, which simulates the oil-brine and rock-brine interfaces reactions.
3. Zeta potential, calcite surface species and current calcite moles are imported into UTCHEM model, which are then used to compute wettability interpolant for relative permeability calculation. Also, PHREEQCRM calculated elements concentrations are imported into UTCHEM to update its brine concentration.
4. With the recalculated relative permeability for each grid-block, the next time step is simulated and produces new ion concentrations.
5. The procedure repeats until the final time-step, consistent with the experimental data is reached

It is worth noting that only aqueous components are modified at each time step, as PHREEQCRM calculated number of moles of mineral and surface species are saved automatically at each time step [78,89]. For PHREEQCRM and UTCHEM to have equivalent volume of solution (V_{H_2O}), UTCHEM grid block volume (in litres), water saturation and porosity are used in PHREEQCRM to calculate V_{H_2O}. Total hydrogen, total oxygen, and charge imbalance are also transferred to PHREEQCRM.

The current number of moles of mineral α, n_α^t (in moles) retrieved from PHREEQCRM is used to calculate and update UTCHEM porosity. The dissolution effect on porosity is calculated as:

$$\varphi_t = \varphi_{t-1} + \left(\frac{\sum dn_\alpha V_{m\alpha}}{V_b}\right) \tag{4}$$

$$dn_\alpha = n_\alpha^{t-1} - n_\alpha^t \tag{5}$$

where V_b is bulk volume of the grid block, and $V_{m\alpha}$ is molar volume of mineral α $\left(\frac{\text{L}}{\text{mol}}\right)$. n_α^{t-1} is number of moles of mineral α in previous time step (in moles), and dn_α is the reacted moles of mineral α. dn_α is positive when mineral dissolution occurs, but negative when the mineral precipitates. However, if neither dissolution nor precipitation occurs, dn_α is 0. Likewise, absolute permeability is calculated as [90–92]:

$$K_t = K_{t-1}\left(\frac{\varphi_t^3}{(1-\varphi_t)^2}\right)\left(\frac{(1-\varphi_{t-1})^2}{\varphi_{t-1}^3}\right) \tag{6}$$

where φ_t is current porosity, φ_{t-1} is porosity in the previous time step. K_t is current permeability, and K_{t-1} is permeability in the previous time step . The UTCHEM-PHREEQCRM coupled model was verified before using it to simulate LSWF. The verification process including result, is provided in Boampong et al. [75].

2.3. Wettability alteration model

The WI was developed following the approach of Bonto et al. [71,73] and Goldberg et al. [93,94]. Consider the adsorption reaction of aqueous ion (eg: H^+) to a mineral surface (eg: >SOH):

$>SOH + H_{(s)}^+ <=> >SOH_2^+$ (7).

The intrinsic equilibrium constant, K_{int}, for reaction (7) is given below:

$$K_{int} = \frac{\left[\right\rangle SOH_2^+]}{[\rangle SOH]\left[H_{(s)}^+\right]} \tag{8}$$

However, the concentration of the adsorbing ion at the mineral surface (i.e., $H_{(s)}^+$) is related to the concentration of the ion in the aqueous phase [95,96]:

Table 2
Rock-brine interface reaction parameters [75]. Z0, Z1 and Z2 are change in charge at the 0-plane, IHP, and OHP, respectively.

No.	Calcite-Brine Surface Reactions	log-K at:	25 °C	65 °C	120 °C	Z0	Z1	Z2
8	$>CaOH^{-0.75} + H^+ \Leftrightarrow >CaOH_2^{+0.25}$	11.8	10.82	9.89	1	0	0	
9	$>CaOH^{-0.75} + CO_3^{-2} \Leftrightarrow > CaCO_3^{-1.75} + OH^-$	1.25	1.35	1.5	−0.04	−0.96	0	
10	$>CaOH^{-0.75} + SO_4^{-2} \Leftrightarrow > CaSO_4^{-1.75} + OH^-$	2.47	2.86	3.1	0.44	−1.44	0	
11	$>CaOH_2^{+0.25} + Cl^- \Leftrightarrow > CaOH_2^{+0.25}$ ……Cl^-	−1.1	−3.35	−5.4	0	0	−1	
12	$>CO_3H^{+0.75} \Leftrightarrow > CO_3^{-0.25} + H^+$	−3.54	−3.0	−3.0	−1	0	0	
13	$>CO_3H^{+0.75} + Ca^{+2} \Leftrightarrow > CO_3Ca^{+1.75} + H^+$	−2.9	−2.35	−1.3	−1	2	0	
14	$>CO_3H^{+0.75} + Mg^{+2} \Leftrightarrow > CO_3Mg^{+1.75} + H^+$	−2.9	−2.15	−1.27	−1	2	0	
15	$>CO_3^{-0.25} + Na^+ \Leftrightarrow >CO_3^{-0.25}$ ……Na^+	−1.15	−2.1	−2.7	0	0	1	
16	C1, F/m^2	2.8						
17	C2, F/m^2	4.5						
Mineral dissolution/precipitation reaction								
Reactions	**Log-Keq at 25 °C**							
18	Calcite $\Leftrightarrow Ca^{+2} + CO_3^{-2}$	−8.48[b]						
19	Dolomite $\Leftrightarrow Ca^{+2} + Mg^{+2} + 2CO_3^{-2}$	−17.09[b]						
20	Anhydrite $\Leftrightarrow Ca^{+2} + SO_4^{-2}$	−4.3064[b]						

[b] mineral dissolution/precipitation equilibrium constants are obtained from the database "Phreeqc.dat".

$$\left[H^{+}_{(s)}\right] = \left[H^{+}_{(aq)}\right] \times exp\left[\frac{-\Delta G_{coul}}{RT}\right] \tag{9}$$

where ΔG_{coul} is the Coulombic interaction, which counts for the electrical work required to transport the $H^{+}_{(aq)}$ from the bulk solution to the mineral surface [73,97,98]. It denotes the energy difference between the two states; the state where $H^{+}_{(aq)}$ is in the bulk solution with a potential of ψ_{bk} and the state where it reaches the mineral surface with a potential of ψ_m. ΔG_{coul} is defined:

$$\Delta G_{coul} = \Delta z_m F \psi_m - \Delta z_{bk} F \psi_{bk} \tag{10}$$

$$\Delta G_{coul} = F(\Delta z_m \psi_m - \Delta z_{bk} \psi_{bk}) \tag{11}$$

where Δz_m denotes the charge change at the mineral surface, and Δz_{bk} corresponds to the charge change at the solution phase. According to Equation (8) – (11),

$$K_{int} = \frac{[\rangle SOH^{+}_{2}]}{[\rangle \mathrm{SOH}][H^{+}_{(aq)}]} \times exp\left[\frac{F(\Delta z_m \psi_m - \Delta z_{bk} \psi_{bk})}{RT}\right] \tag{12}$$

Equation (12) can be rearranged as:

$$\frac{\left[H^{+}_{(aq)}\right]}{[\rangle SOH^{+}_{2}]} = \beta_{i,} = \frac{exp\left[\frac{F(\Delta z_m \psi_m - \Delta z_{bk} \psi_{bk})}{RT}\right]}{K_{int}[\rangle \mathrm{SOH}]} \tag{13}$$

where i denotes reaction i; β_i is the wettability indicator, and it corresponds to the ratio of concentration of the ion in the aqueous phase to its adsorbed concentration at the mineral surface. It is a measure of the interaction between the mineral and the fluid [99], and that, large value of β_i implies that less amount of the ion is adsorbed at the mineral surface. Generally, the magnitude of β_i is a function of both the rock and the fluid chemistry [99]. For instance, mineralogy of the rock, ionic strength, pH, and solution composition affect the β_i [100]values. For carbonate-oil-brine interactions, β_i is also affected by the oil composition. It should be noted that, for aqueous ion adsorption, ψ_{bk} is assumed to be zero [97] since the ζ-potential approaches zero in the bulk solution.

Regarding the carbonate-oil-brine system, calcite and oil species interact such that oil species gets adsorbed at the calcite surface. Following Bonto et al. [71,73], the oil-brine and the rock-brine interfaces are treated separately, and the adsorption of oil species occurs at the rock-brine OHP. Therefore, the adsorbing oil species must travel through the oil-brine interface to reach the rock surface. Analogously, Equation (13) can be applied to the oil species reacting with the mineral surface. Accordingly, the parameters in Equation (13) can be defined as: $\Delta z_m = \Delta z_{2,rb}$; $\Delta z_{bk} = \Delta z_{2,ob}$; $\psi_m = \psi_{rb}$; $\psi_{bk} = \psi_{ob}$. Then, Equation (13) is written as:

$$\beta_i = \frac{exp\left[\frac{F\left(\Delta z_{2,rb}\psi_{rb} - \Delta z_{2,ob}\psi_{ob}\right)}{RT}\right]}{K_{int}[\rangle \mathrm{SOH}]} \tag{14}$$

Following Appello & Postma [97], K_{int} is assumed as constant value. Hence, Equation (14) reduces to:

$$\beta_i = \frac{exp\left[\frac{F\left(\Delta z_{2,rb}\psi_{rb} - \Delta z_{2,ob}\psi_{ob}\right)}{RT}\right]}{[\rangle \mathrm{SOH}]} \tag{15}$$

$$\Delta z_{2,ob} = -1 \times j \tag{16}$$

where $\Delta z_{2,rb}$ denotes the charge change at the rock-brine OHP, following the adsorption reaction i; $\Delta z_{2,ob}$ is the charge change at the oil-brine OHP, following the adsorption reaction i. Also, ψ_{rb} corresponds to the potential at the rock-brine OHP, which is assumed to be equivalent to ζ-potential (in Volts); ψ_{ob} denotes potential at the oil-brine OHP, which is assumed to be equivalent to the ζ-potential (in Volts), and j represents the charge of the adsorbing oil species. For instance, for the adsorption of the COO^{-} oil species, j = -1. [> SOH] denotes the concentration of calcite surface group reacting with the oil species in reaction i (eg: $>CO_3^{-0.25}$), in mol/m^2. Accordingly, β_i relates the concentration of the free oil phase to the adsorbed oil concentration at the calcite surface. Large value of β_i implies low oil adsorption and more oil recovery. Amount of the surface species, [⟩SOH], can be expressed in number of moles. Equation (16) then becomes:

$$\beta_i = \frac{exp\left[\frac{F\left(\Delta z_{2,rb}\psi_{rb} - \Delta z_{2,ob}\psi_{ob}\right)}{RT}\right]}{[\rangle \mathrm{SOH}] \times SSA \times mass_{calcite}} \tag{17}$$

$$\beta_i = \frac{exp\left[\frac{F\left(\Delta z_{2,rb}\psi_{rb} - \Delta z_{2,ob}\psi_{ob}\right)}{RT}\right]}{[\rangle \mathrm{SOH}] \times SSA \times M_{calcite} \times n_{calcite}} \tag{18}$$

where $M_{calcite}$ is molecular weight of calcite in g/mol (constant); $n_{calcite}$ corresponds to the amount of calcite in mol, and SSA is specific surface area of calcite, m^2/g (constant). From the above equation, it can be observed that β_i is related to the values of [⟩SOH], $n_{calcite}$, and the exponential term. Essentially, concentration of the calcite surface group [> SOH] reacting with the oil components serves as a limiting factor for β_i, controlling the amount of oil adsorbed on the rock surface [73]. Dissolution of calcite mineral will increase β_i, whiles the effect of oil-brine and rock-brine interface ζ-potentials on β_i will depend on the polarities and magnitudes of the ζ-potentials. Relative permeability interpolant, β^{int}_{total}, is then calculated as:

$$\beta^{int}_{i} = \frac{\beta^{t}_{i} - \beta^{final}_{i}}{\beta^{initial}_{i} - \beta^{final}_{i}} \tag{19}$$

$$\beta^{int}_{total} = \sum_{i}^{n} {\omega_\sigma}^{t} \beta^{int}_{i} \tag{20}$$

$${\omega_\sigma}^{t} = \frac{\left[> SOH_{\sigma,i}\right]^{t}}{\left[> C_{total}\right]^{t}} \tag{21}$$

where $\left[> SOH_{\sigma,i}\right]$ is the concentration of calcite surface species σ in reaction i, and $[> C_{total}]$ denotes total concentration of calcite surface species which reacted with the oil. $\beta^{initial}_{i}$ is the value for reaction i calculated at the initial conditions of brine salinity, β^{final}_{i} is the value for reaction i calculated at the final state, and β^{t}_{i} is the value calculated at the current time step. ω_σ corresponds to weight factor of the calcite surface species σ involved in the carbonate-oil-brine reactions, and t is current simulation time step. The values of β^{int}_{total} is between the range of one and zero, and that the initial wettability remains unaltered when the value of β^{int}_{total} is zero. However, the wettability reaches the final state (i.e., moves towards a more water-wet state) when the value of β^{int}_{total} approaches zero.

Identification of the correct carbonate-oil-brine adsorption reaction (s) responsible for the WI is required. Several calcite-oil adsorption reactions have been proposed by various investigators. For instance, Bonto et al. [71,73] suggested that carbonate wettability is controlled predominantly by the acid/base interactions. Hence, they used the reaction between $> CaOH_2^{+0.333}$ and COO^{-}; $> CO_3^{-0.333}$ and NH^{+} in their developed WI for LSWF studies. Brady et al. [8] also proposed that the electrostatic linkages of $> CaOH_2^{+}$ and COO^{-}, and $> CO_3^{-}$ and NH^{+} are dominants. They further explained that the presence of Ca^{+2}, Mg^{+2} and SO_4^{-2} ions in brine can affect the electrostatic linkage. That is, SO_4^{-2} adsorption at the carbonate surface can reduce $> CaOH_2^{+}$ sites whereas Ca^{+2}, Mg^{+2} adsorptions can reduce COO^{-} sites at the oil surface.

Ding et al. [101], however, attributed crude oil adsorption to the combination of acid/base interactions and ion-binding interactions. That is, the reactions between: $> CaOH_2^{+}$ and COO^{-}, $> CO_3C_a^{+1.75}$ and COO^{-}, $> CO_3M_g^{+1.75}$ and COO^{-}. Laboratory studies conducted on LSWF usually involve saturating the core with water before displacing it with

oil (to obtain initial condition). Therefore, polar interactions are excluded from the carbonate-oil-brine interactions in our model. Surface precipitation interactions can also be ignored when the oil contains small asphaltenes [6]. Based on Qiao et al. [6], acid/base and ion-binding interactions are assumed to dominate the carbonate-oil-brine interactions. Consequently, two models are considered in this study (Table 3). Model 1 assumes that wettability is controlled by both acid/base and ion-binding interactions whereas model 2 uses only acid/base interactions. Only one of the proposed two models is applied at a time in our simulation. Hence, model 1 is always considered first in the LSWF calculations, however, where it fails to predict the oil recovery trend, model 2 is used.

Corey's end-point relative permeabilities and exponents are then interpolated as:

$$K_{ro}^{o} = \beta_{total}^{int} K_{ro}^{hsw} + \left(1 - \beta_{total}^{int}\right) K_{ro}^{lsw} \tag{22}$$

$$K_{rw}^{o} = \beta_{total}^{int} K_{rw}^{hsw} + \left(1 - \beta_{total}^{int}\right) K_{rw}^{lsw} \tag{23}$$

$$n_o = \beta_{total}^{int} n_o^{hsw} + \left(1 - \beta_{total}^{int}\right) n_o^{lsw} \tag{24}$$

$$n_w = \beta_{total}^{int} n_w^{hsw} + \left(1 - \beta_{total}^{int}\right) n_w^{lsw} \tag{25}$$

Reduction in the residual oil saturation due to the LSWF effect was also interpolated:

$$S_{or} = \beta_{total}^{int} S_{or}^{ow} + \left(1 - \beta_{total}^{int}\right) S_{or}^{ww} \tag{26}$$

where K_{ro}^{lsw} denotes the end-point relative permeability to oil at final state, where the total concentration of the pore-space aqueous phase is reduced to the salinity of the injected low salinity water (final low salinity water condition), K_{ro}^{hsw} is end-point relative permeability to oil at initial brine condition (FW condition) and K_{ro}^{o} is the current end-point relative permeability to oil. K_{rw}^{lsw} corresponds to the end-point relative permeability to water at final low salinity water condition,K_{rw}^{hsw} is end-point relative permeability to water at initial brine condition, and K_{rw}^{o} is current end-point relative permeability to water. n_o^{hsw} is Corey's oil exponent at initial brine condition, n_o^{lsw} is Corey's oil exponent at low salinity water condition, and n_o is the current Corey's exponent for oil. n_w^{hsw} is Corey's water exponent at initial brine condition, n_w^{lsw} is Corey's water exponent at low salinity water condition, and n_w is the current Corey's exponent for water. S_{or}^{lsw} corresponds to residual oil saturation at low salinity water condition, S_{or}^{hsw} is residual oil saturation at initial brine condition, and S_{or} denotes current residual oil saturation. Relative permeability to water (K_{rw}) and oil (K_{ro}) during the LSWF process is finally calculated from Brooks and Corey's correlation:

$$K_{rw} = K_{rw}^{o}(S_n)^{n_w} \tag{27}$$

$$K_{ro} = K_{ro}^{o}(1 - S_n)^{n_o} \tag{28}$$

$$S_n = \frac{S_w - S_{wc}}{1 - S_{wc} - S_{or}} \tag{29}$$

2.4. Model validation

We tested the developed WI against the experimental LSWF tests of Chandrasekhar & Mohanty [67], Yousef et al. [27], and Austad et al. [36]. These studies reported the dissolution, ion exchange, and surface charge (i.e., ζ-potentials) wettability alteration mechanisms, and hence, our new WI model can capture them. The experimental data from these studies is given in Table 4 and Table 5. Furthermore, sensitivity studies were conducted using the model to find the optimum salinity of the low salinity brine to inject, the time to inject the low salinity water, and the effect of injection rate on LSWF.

3. Results

This section presents results of simulations performed with the model. It should be noted that validation of the TLM with experimental data is provided in Boampong et al. [75]. This was achieved by using the TLM to calculate oil-brine and rock-brine interface ζ-potentials and compared the results with experimental data sets. Here, we present results of the oil recovery calculated with the developed WI model. It should be noted that all simulations were performed using a one-dimension model.

3.1. Validation of the model with experimental oil recovery

Typically, relative permeability curves are measured in the laboratory at the end-point wetting states. However, the simulated LSWF experiments did not report relative permeability and capillary pressure curves. Consequently, relative permeability end points were estimated from the best fit to the experimental oil recoveries. To reduce the number of tuning parameters, capillary pressure was assumed to be zero.

Table 4
Properties of rock and oil used by the authors.

Property	**Austad** et al. [36]	**Yousef** et al. [27]	**Chandrasekhar & Mohanty** [67]
Porosity, fraction	0.25	0.25	13.6, 15.4
Permeability, mD	51	39.6	17, 10
Diameter, cm	3.8	3.8	7.4, 7.6
Length, cm	8.4	16.24	3.8
Initial Water saturation, fraction	0.1	0.104	0.16, 0.24
1Initial Pressure, bar	10	13.8	5.17
Reservoir Temperature, °C	100	100	120
Injection rate, cm^3/min	0.01	1	0.045
TAN, mg KOH/g oil	0.15	0.25	2.45
TBN, mg KOH/g oil	0.84	–	–
Oil density, g/cm^3	0.875 at 25 °C	0.72 at 100 °C	0.82 at 25 °C
Oil viscosity, cp	19.9 at 25 °C	2.03 at 100 °C	1.05 at 120 °C

Table 3
Carbonate-oil adsorption reactions considered in the model.

Reaction	**Model 1**	$\Delta z_{2,rb}$	$\Delta z_{2,ob}$	ω_σ
1	$>CaOH_2^{+0.25} + COO^- \quad > CaOH_2\ldots COO^{+0.75}$	−1	1	$[\rangle CaOH_2^{+0.25}/>C_{total}]$
2	$>CO_3^{-0.25} + NH^+ \quad > CO_3\ldots NH^{+0.75}$	1	−1	$[\rangle CO_3^{-0.25}/>C_{total}]$
3	$>CO_3Ca^{+1.75} + COO^- \quad > CO_3Ca\ldots COO^{+0.75}$	−1	1	$[\rangle CO_3Ca^{+1.75}/>C_{total}]$
4	$>CO_3Mg^{+1.75} + COO^- \quad > CO_3Mg\ldots COO^{+0.75}$	−1	1	$[\rangle CO_3Mg^{+1.75}/>C_{total}]$
where:	$[\rangle C_{total}] = [\rangle CaOH_2^{+0.25} + >CO_3^{-0.25} + >CO_3Ca^{+1.75} + >CO_3Mg^{+1.75}]$			
Model 2				
5	$>CaOH_2^{+0.25} + COO^- \quad > CaOH_2\ldots COO^{+0.75}$	−1	1	$[\rangle CaOH_2^{+0.25}/>C_{total}]$
6	$>CO_3^{-0.25} + NH^+ \quad > CO_3\ldots NH^{+0.75}$	1	−1	$[\rangle CO_3^{-0.25}/>C_{total}]$
where:	$[\rangle C_{total}] = [\rangle CaOH_2^{+0.25} + >CO_3^{-0.25}]$			

Table 5
Composition of brines used by the authors. For SW0Na, concentration of NaCl in SW is removed.

Austad et al. [36], **mmol/l**								
Brine/ion	Na^+	Ca^{2+}	Mg^{2+}	SO_4^{2}	Cl^-	K^+	HCO_3^-	**TDS**
FW	2577.1	475	100	0	3721.1	0	6	213 (g/l)
SW	797.5	16	86	45	909.5	0	2	57.76 (g/l)
SW0Na	92	16	86	45	204	0	2	16.53 (g/l)
Yousef et al. [27], **ppm**								
FW	59,491	19,040	2349	350	132,060	0	354	213,734 (ppm)
SW	18,300	650	2110	4290	32,200	0	120	57,670 (ppm)
Chandrasekhar & Mohanty [67], **ppm**								
FW	49,933	14,501	3248	234	111,810	0	0	149,160 (mg/l)
SW	13,700	521	1620	3310	24,468	0	0	41,127 (mg/l)

It is noteworthy that WI model 1 was used in calculating the wettability indicator for all the simulations in this section.

3.1.1. *Modelling of Chandrasekhar & Mohantyl [67] LSWF experiment*

Chandrasekhar & Mohanty [67] performed LSWF tests in limestone core consisting predominantly of calcite (>98 % calcite). They studied the dilution effect on LSWF by injecting two diluted brines: SW/20 and SW/50 at tertiary stages, where SW/20 and SW/50 signify seawater diluted 20 times and 50 times, respectively. For each injection cycle, FW was injected at the secondary stage followed by the low salinity water. For experiment 1, referred to as CF10, injection of FW at secondary stage recovered 40 % of the original oil in place (OOIP), where SW/20 produced additional 40 % of OOIP at the tertiary injection. During experiment 2 (CF11), FW produced 40 % of the OOIP at secondary stage with additional 34 % recovered by SW/50 injection.

The experimental results were simulated with our developed model. The oil acid site-density (26.3/nm^2) was calculated from the reported TAN of 2.45 mg KOH/g oil. The base site-density was assumed to be equivalent to the acid site-density because the TBN was not reported by the authors. Following Chandrasekhar et al. [102], we assumed that the rock is initially composed of only calcite as the initial dolomite amount is insignificant. However, dolomite and anhydrite precipitation were considered in the model. This is because the brines used by Chandrasekhar & Mohanty [67] contained significant amount of Ca^{+2}, Mg^{+2}, and SO_4^{2} ions, where mineral precipitation is possible. The optimized relative permeabilities end points and Corey's exponents used to predict the results are shown in Table 6.

Fig. 1 and Fig. 2 compare the oil recoveries and effluent ions calculated by the model with the experimental data, where good matches are obtained between the outputs of the model and the experimental tests.

The wettability indicator produced by the model showed smaller WI values calculated at the FW injection, which shifted to larger values during the LSWF (Fig. 3a). It should be noted that WI is the ratio of the concentration of free oil to the concentration of adsorbed oil. Hence, an increase in WI corresponds to the desorption of oil from the mineral surface (i.e., high amount of the free oil), signifying improved oil recovery. At the initial condition of FW (and until the end of FW injection), significant amount of the carboxylic oil component was adsorbed at the carbonate rock surface, and this is shown by the smaller carboxylic oil associated WI values. That is, a considerable amount of the adsorbed oil occurred from the reaction between the carboxylic oil component and the calcite positive surface species ($>CaOH_2^{+0.25}$, $>CO_3Ca^{+1.75}$, $>CO_3Mg^{+1.75}$). On switching the injection brine to the low salinity water (SW/20), the carbonate-oil-brine reactions resulted in the desorption of the carboxylic oil group from the mineral surface. Consequently, the carboxylic oil related WI is observed to be increasing, with the $>CO_3Ca\_COO$ component dominating the other components. Conversely, the calculated WI for the $>CO_3\_NH$ group can be seen to be decreasing during the low salinity water injection. Our model outcomes are consistent with the simulation results reported in the literature [103]. Sharma & Mohanty [103] noted a reduction in the concentration of the adsorbed acidic oil components when the low salinity water was injected. They proposed that the low salinity water liberated the oil from the carbonate $>CaOH_2^{+0.25}$, $>CO_3Ca^{+1.75}$, and $>CO_3Mg^{+1.75}$ sites, and this increased the oil recovery. Fig. 3b shows that the β_{total}^{int} moves towards zero when the low salinity water was injected, signifying a shift in the wettability towards a more water-wet state. The residual oil saturation decreases as the β_{total}^{int} moves towards zero.

Table 6
Relative permeability parameters used to simulate Chandrasekhar & Mohanty [67] experiments.

Parameter FW & SW/20	**Initial value**	**Final value**
S_{wc}	0.16	0.16
S_{or}	0.52	0.15
K_{row}	0.2	0.2
K_{rw}	0.2	0.15
n_w	2	3
n_o	3	2.5
FW & SW/50		
S_{WC}	0.24	0.24
S_{or}	0.46	0.19
K_{row}	0.2	0.2
K_{rw}	0.2	0.15
n_w	2	3
n_0	3	2.5

The calculated oil-brine and rock-brine interface ζ-potentials show positive ζ-potential values for the FW injection (Fig. 4). The ζ-potential values are noted to have shifted to negative values during the LSWF. Additionally, magnitude of the LSWF produced ζ-potentials exceeded the FW injection ζ-potentials.

Calcite dissolution was not observed in the model, as the initial amount of calcite remained unchanged during the injection period (Fig. 5a). It was further observed that the WI calculated for SW/50 injection is larger than the WI calculated for the SW/20 injection (Fig. 5b). Therefore, one would expect the injected SW/50 to recover more additional oil than the SW/20. Interestingly, Chandrasekhar & Mohanty [67] produced more incremental oil at the SW/20 injection (incremental 40 % OOIP) than the SW/50 injection (incremental 34 % OOIP). This is due to the petrophysical properties of the cores used for the two experiments, and we discuss the details of this phenomena in the next section.

3.1.2. *Modelling of Austad et al. [36] LSWF experiment*

Our next simulated data is the LSWF experiment conducted by Austad et al. [36]. In their tertiary LSWF experiment, FW was injected at the secondary stage which was followed by the subsequent injections of low salinity water. That's, the seawater was injected after the FW injection, which is followed by the injection of the seawater depleted of NaCl. The limestone core used for the study was composed of calcite and small amount of anhydrite [36]. Austad et al. [36] reported the TAN and TBN of 0.15 mg KOH/g oil and 0.84 mg KOH/g oil, respectively.

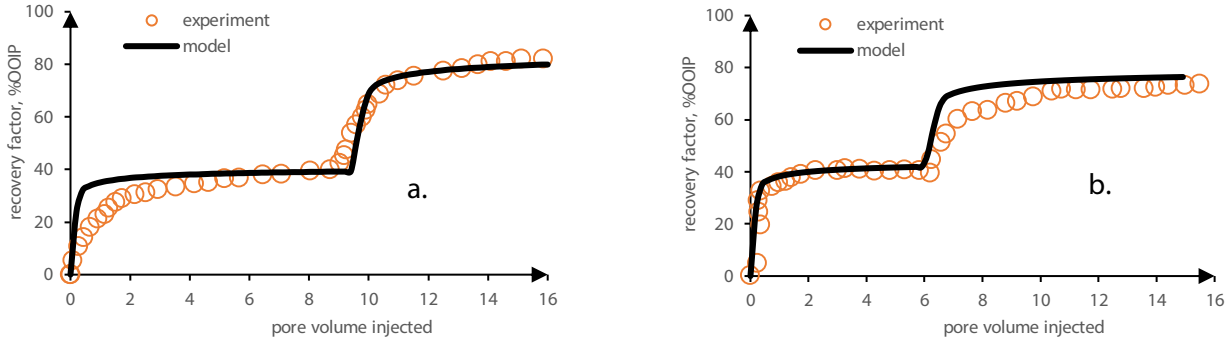

Fig. 1. History match of model (this study) to Chandrasekhar & Mohanty [67] oil recovery data. (a) FW => SW/20 flood match, and (b) FW => SW/50 flood match.

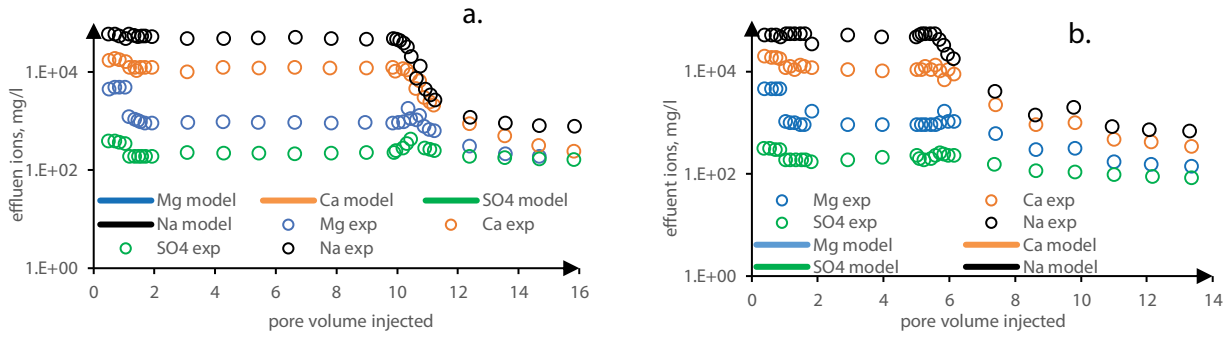

Fig. 2. Effluent ion match (a) FW=>SW/20 flood, (b) FW=>SW/50 flood.

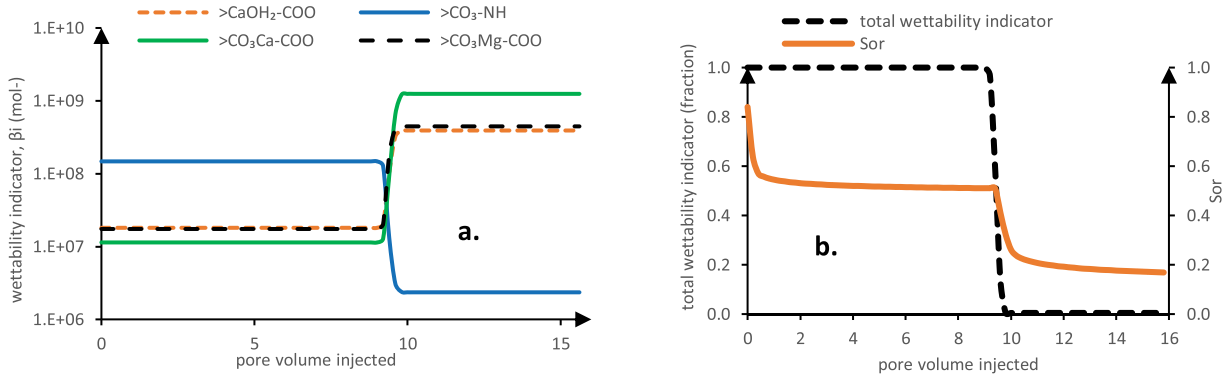

Fig. 3. (a) Calculated wettability indicator (β_i^{int}) for the brine injections, and (b) relationship between total wettability indicator (β_{total}^{int}) and residual oil saturation during the brine injections. Residual oil saturation decreases as β_{total}^{int} moves towards zero.

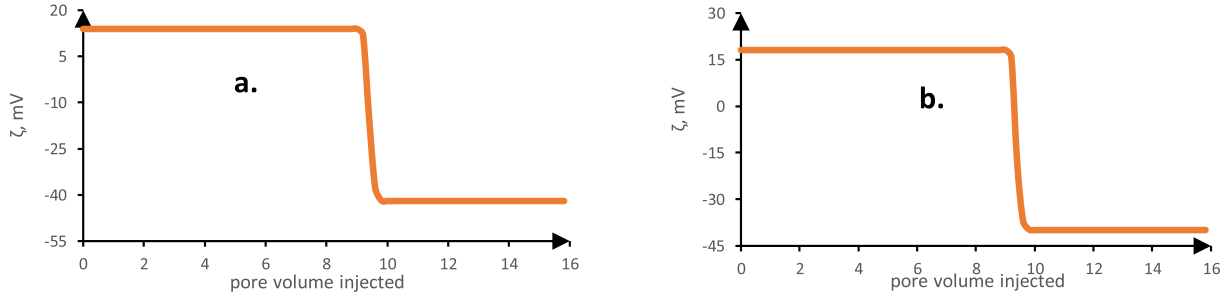

Fig. 4. Calculated ζ-potentials for the carbonate-oil-brine system. (a) rock-brine interface ζ-potentials, and (b) oil-brine interface ζ-potentials.

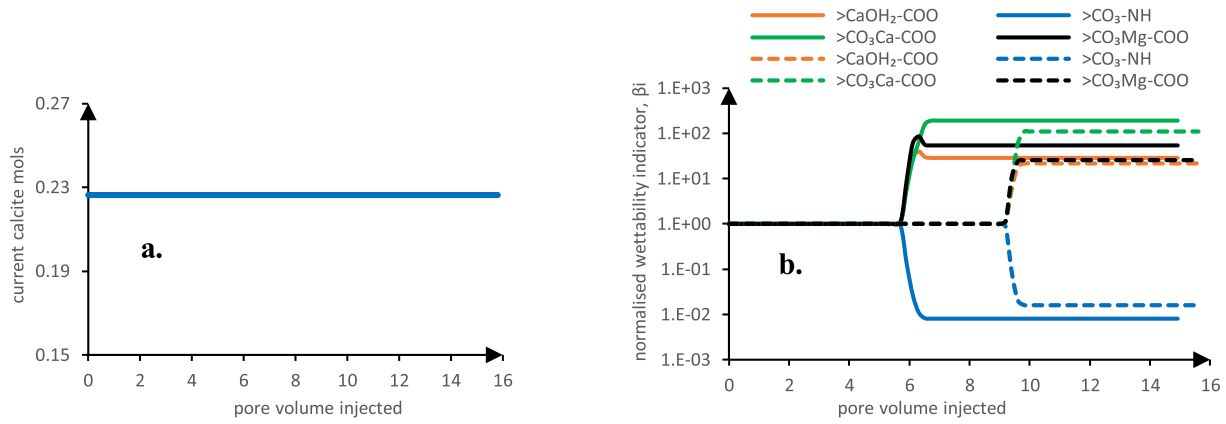

Fig. 5. (a) calculated calcite moles, and (b) calculated normalised wettability indicator: dash lines denote the SW/20 WI values and the solid lines for SW/50 WI values.

Table 7
Relative permeability parameters used to simulate Austad et al. [36] experiment.

Parameter	Initial value	Final value
S_{wc}	0.1	0.1
S_{or}	0.72	0.63
K_{row}	0.2	0.2
K_{rw}	0.5	0.4
n_w	2	2
n_o	3	2

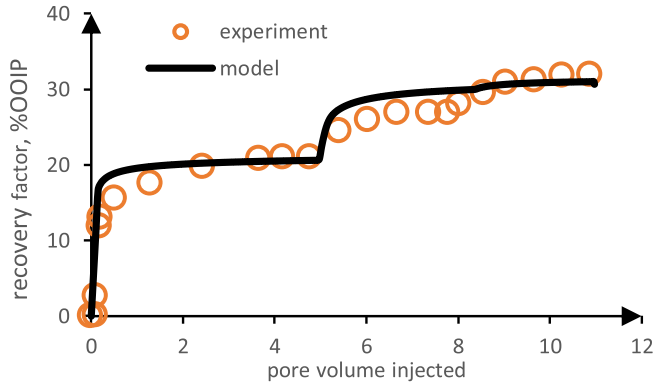

Fig. 6. History match of model (this study) to Austad et al. [36] oil recovery data.

Applying Equation (1) and (2), calculated acid and base site-densities of 1.61/nm^2 and 9.01/nm^2, respectively, were obtained. Table 7 shows the optimized relative permeability values used to predict the experimental results.

Fig. 6 depicts the oil recovery factor calculated by the model that matched the experimental results. Fig. 7a shows that a considerable amount of the carboxylic oil component was initially adsorbed at the mineral surface, and this is indicated by the low carboxylic oil related WI values obtained at the initial reservoir condition. Desorption of the carboxylic oil component happens during the low salinity water injections. This is exhibited by the high carboxylic oil related WI values calculated at the low salinity water injections, where the > CO_3Ca_COO component dominates. On the other hand, the calculated WI for the > CO_3_NH group decreased during the low salinity water injections. No substantial increase is observed in the calculated > CO_3Mg_COO WI values for the duration of the low salinity water injection. Desorption of the oil from the rock surface improved the oil recovery factor. The residual oil saturation is identified to be decreasing as the β^{int}_{total} moves towards zero (Fig. 7b), which implies a shift in the wettability towards a more water-wet state.

The model shows positive ζ-potentials calculated at both oil-brine and rock-brine interfaces during the FW injection (Fig. 8). Nonetheless, switching the brine to the low salinity water produced negative ζ-potentials at the rock-brine and the oil-brine interfaces. Similar to the previous results, there is no observation of calcite dissolution in the simulation results (Fig. 9).

3.1.3. *Modelling of Yousef et al. [27] LSWF experiment*

The proposed model was used to simulate the core flooding results of Yousef et al. [27], and a good match was achieved (Fig. 10). The

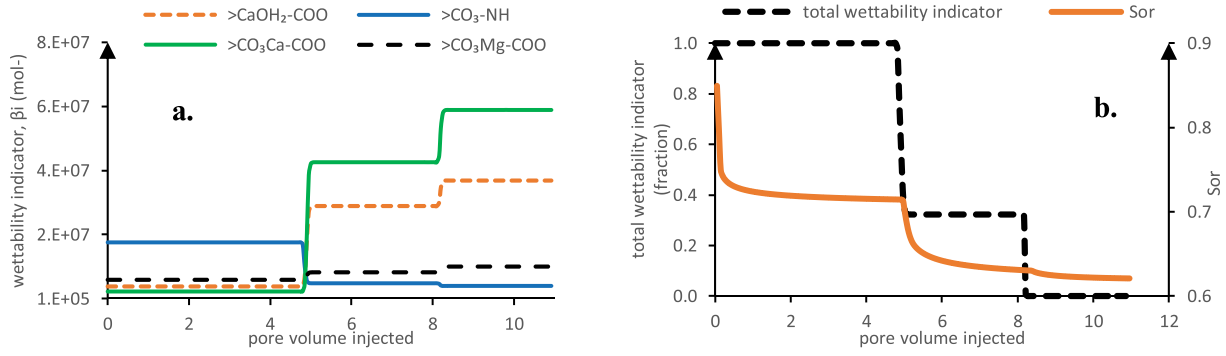

Fig. 7. (a) Calculated wettability indicator (β_i^{int}) for the brine injections, and (b) relationship between total wettability indicator (β_{total}^{int}) and residual oil saturation during the brine injections. Residual oil saturation decreases as β_{total}^{int} moves towards zero.

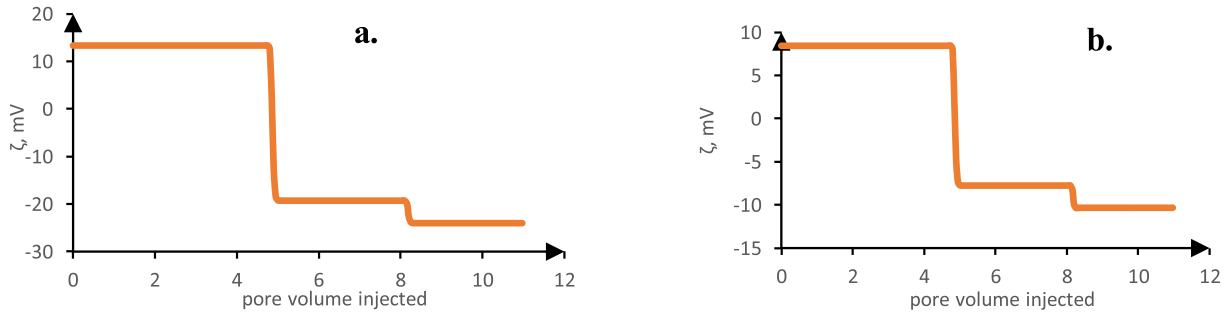

Fig. 8. Calculated ζ -potentials for the carbonate-oil-brine system. (a) rock-brine interface ζ -potentials, and (b) oil-brine interface ζ -potentials.

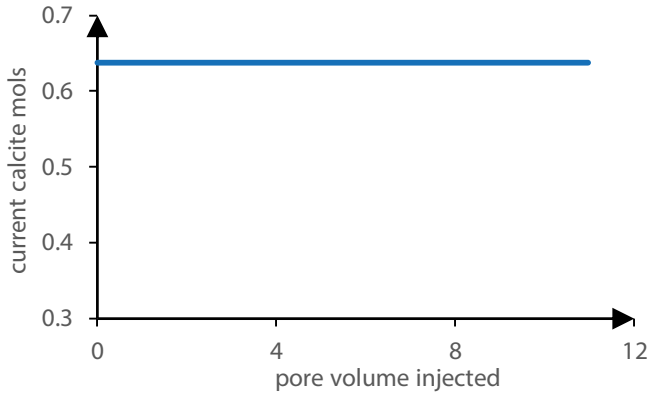

Fig. 9. Calculated calcite amount.

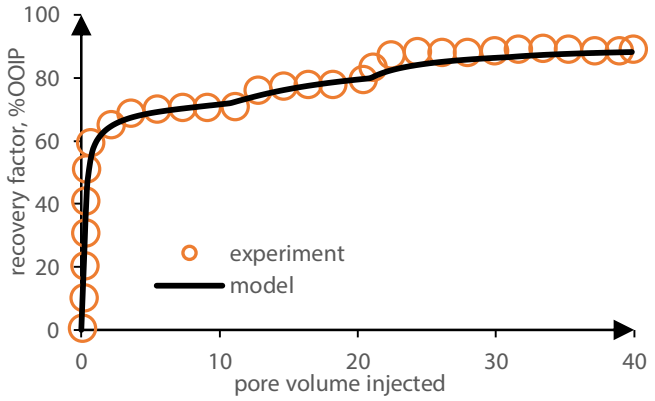

Fig. 10. History match of model (this study) to Yousef et al. [27] first core flood oil recovery data.

carbonate rock used by these investigators was reported to compose of calcite, dolomite, and anhydrite [15]. Yousef et al. [27] studied LSWF process by injecting SW at secondary stage, followed by successive injections of the diluted SW; twice diluted (SW/2) ten times diluted (SW/10), twenty times diluted (SW/20), and hundred times diluted (SW/100). We calculated acid site-density of 2.69/nm^2 from the reported TAN (0.25 m^2 KOH/g oil) and assumed the same number for the base site-density because TBN was not reported. The optimized relative permeabilities used to predict the experimental results are shown in Table 8. It is noteworthy that the end point relative permeability values used for the current simulation is different from the end point values used in the previous study [75]. We earlier indicated that the current WI is more robust, as it captures more of the oil adsorption/desorption mechanisms. Therefore, the current end point relative permeability values are proposed to be more accurate than the end point values used in the previous study [75].

Table 8
Relative permeability parameters used to simulate Yousef et al. [27] experiment.

Parameter	Initial value	Final value
S_{wc}	0.1044	0.1044
S_{or}	0.33	0.12
K_{row}	0.27	0.27
K_{rw}	0.3	0.28
n_w	2	3
n_o	2.2	1.8

A similar trend was observed from the calculated WI values (Fig. 11a). The injection of the diluted seawater resulted in increased calculated WI for the > $CaOH_2$_COO, >CO_3Ca_COO, and > CO_3Mg_COO components. This implies desorption of the adsorbed COO^- group from the carbonate surface, increasing the oil recovery. Contributions from the > $CaOH_2$_COO, >CO_3Ca_COO, and > CO_3Mg_COO components on oil recovery are noticed to be similar, although, the > $CaOH_2$_COO group dominates. The > CO_3_NH calculated WI is however, decreasing with the low salinity water. Fig. 11b shows the calculated β_{total}^{int} shifting towards zero when the low salinity water is injected, indicating desorption of the oil from the carbonate surface (i.e., the wettability is shifted towards a more water-wet state). The residual oil saturation decreases as the β_{total}^{int} moves towards zero.

The calculated oil-brine and rock-brine ζ-potentials are observed to have shifted from positive (at the initial condition) to negative values during SW injection (Fig. 12). The ζ-potentials are continuously becoming negative as the diluted brines are injected. This is consistent with the results reported by Yousef et al. [15]. They obtained negative rock-brine ζ-potential when the carbonate rock was equilibrated with the SW. The ζ-potential then becomes more negative when the SW was diluted ten times, twenty times, and hundred times. Again, the model results did not show any calcite dissolution as the calcite moles remained constant (Fig. 13).

3.2. Sensitivity studies

The performance of LSWF is not only influenced by the mineralogical content of the carbonate rock and the oil properties, but also by other important parameters such as injection rate, optimum dilution of the injection brine, and time to begin the low salinity waterflood [98–101]. Sensitivity studies were conducted using our model to explore the impact of these parameters on wettability alteration and oil recovery. The experimental data of Yousef et al. [27] was employed for this purpose, using our history matched relative permeability values from the previous part.

3.2.1. Time to begin the low salinity waterflood

The injection of low salinity water at a tertiary stage has been extensively studied, however, similar attention is not given to the secondary LSWF. Previous studies on LSWF have shown that injection of the

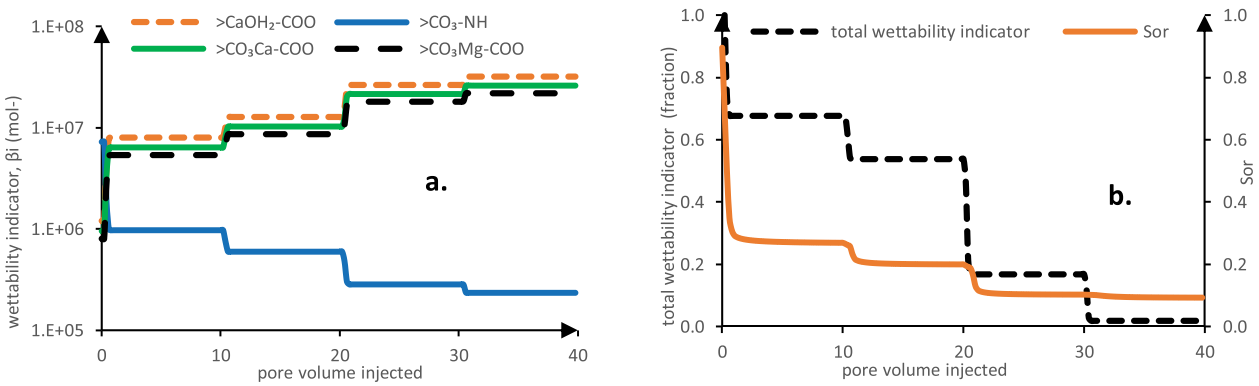

Fig. 11. (a) Calculated wettability indicator (β_i^{int}) for the brine injections, and (b) relationship between total wettability indicator (β_{total}^{int}) and residual oil saturation during the brine injections. Residual oil saturation decreases as β_{total}^{int} moves towards zero.

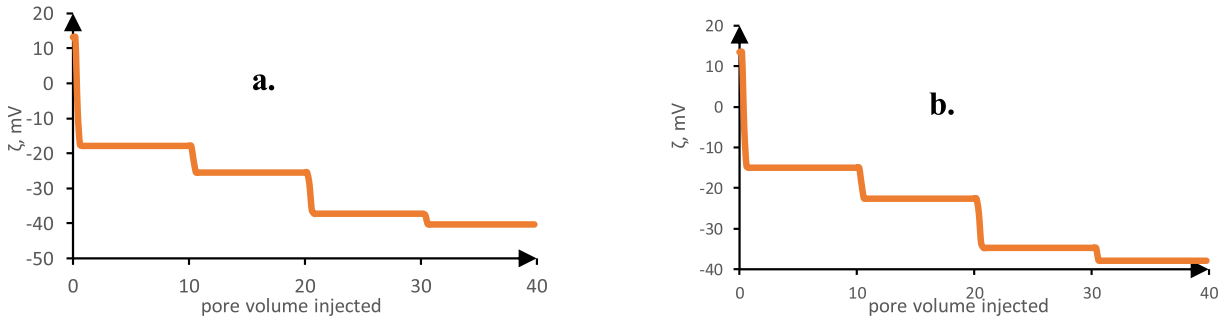

Fig. 12. Calculated ζ-potentials for the carbonate-oil-brine system. (a) rock-brine interface ζ-potentials, and (b) oil-brine interface ζ-potentials.

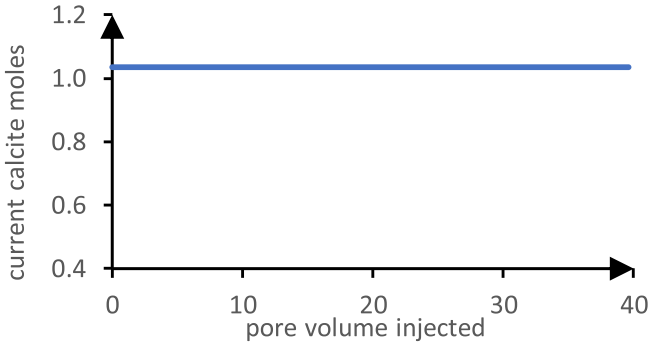

Fig. 13. Calculated calcite amount.

low salinity water in a secondary mode can be more effective than the tertiary injection of the low salinity water [104–107]. Shiran & Skauge [105] reported that using the secondary injection method increased the oil recovery by 13 % OOIP compared to the tertiary injection of the low salinity water. Egbe et al. [104] reported that more oil was produced in their experiments via the secondary injection method than the tertiary injection method. Furthermore, Rivet et al. [107] conducted a series of experiments and found that no significant amount of incremental oil was produced at the tertiary stage.

In this study, simulations were performed for both secondary and tertiary LSWF, using the twice diluted seawater (SW/2) and the ten times diluted seawater (SW/10). Regarding the tertiary LSWF, six pore volumes (6 PV) of the seawater (SW) was first injected at the secondary stage followed by the injection of four pore volumes (4 PV) of the low salinity water (SW/2 or SW/10) at the tertiary stage. Fig. 14 shows the simulation outcomes where higher oil recoveries were achieved from the secondary injection of the low salinity water. For instance,

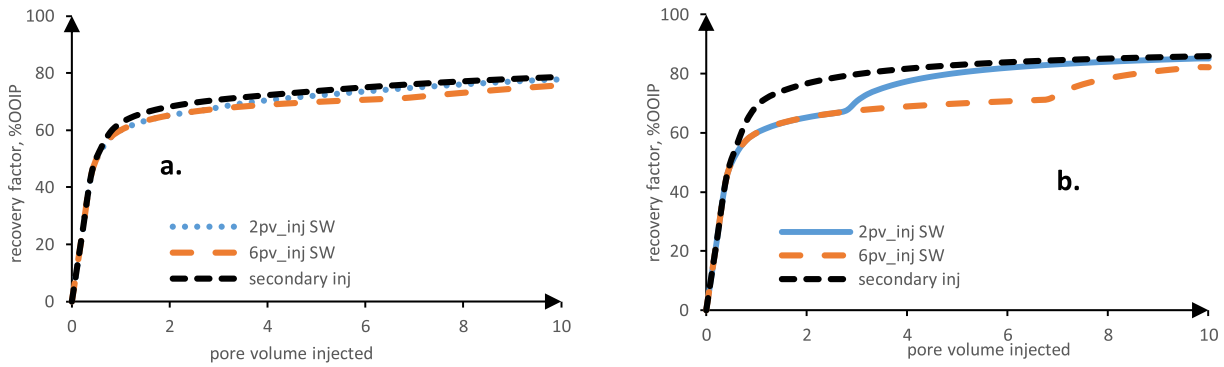

Fig. 14. (a) Tertiary and secondary injection of the SW/2, and (b) tertiary and secondary injection of the SW/10. "2pv_inj SW" denotes tertiary LSWF (2 PV of SW was injected at the secondary stage); "6pv_inj SW" denotes tertiary LSWF (6 PV of SW was injected at the secondary stage). "secondary inj" indicates secondary LSWF.

secondary injection of the SW/2 recovered about 79 % OOIP while injecting the same brine in the tertiary mode reduced the oil recovery by about 3 % OOIP. Also, secondary injection of the SW/10 produced about 86 % OOIP, which was reduced by 4 % OOIP when the same brine was injected in the tertiary mode. We further investigated the tertiary LSWF by injecting only 2 PV of the SW at the secondary stage instead of 6 PV. An increase in the oil recovery was observed from this injection pattern, with the final oil recoveries equivalent to the secondary LSWF oil recoveries. The results suggest that early injection of low salinity water can substantially improve oil recovery in carbonate reservoirs, and the mechanisms behind this behavior (i.e., the early injection giving better oil recoveries) are discussed in the next section (i.e., section 4.6).

3.2.2. *Injection rate*

To understand the impact of injection rate on LSWF, we performed simulations using four different injection rates: 0.1 ml/min, 0.069 ml/min, 0.035 ml/min, and 0.001 ml/min. The SW/2 brine was used for this study, and all the simulations were carried out at the secondary recovery mode. The simulation results showed increased oil recovery with increasing injection rate (Fig. 15a). The 0.1 ml/min injection rate recovered about 90 % OOIP, which is about 15 % OOIP more than the oil produced by the 0.001 ml/min injection rate. The injection rates influenced the wettability indicator, but this occurred during the early stages of the brine injections (i.e., up to about 1.0 PV injections), after which all the injection rates produced similar wettability indicators (Fig. 15b). At 0.4 PV, the calculated total wettability indicator for the 0.001 ml/min rate is 0.57, followed by the 0.035 ml/min injection rates, with total wettability indicator of 0.64. The 0.1 ml/min injection rate produced the highest total wettability indicator of 0.83. This implies that the 0.001 ml/min injection rate produced the highest wettability alteration (shifted the reservoir to a more water-wet condition) at the 0.4 PV, nonetheless, the 0.001 ml/min rate recovered the lowest amount of oil at the 0.4 PV. The mechanisms behind this discrepancy are discussed in the next section (i.e., section 4.6).

3.2.3. *Optimum dilution of the injection brine*

Decreasing the salinity of the injection water can significantly influence the LSWF oil recovery. However, obtaining the optimum brine salinity can be difficult, as multiple laboratory experiments are required to establish the optimum brine salinity, and this can be time consuming and expensive. In laboratory experiments, low salinity water is usually obtained by diluting high salinity brine (e.g., formation or seawater). It is worth pointing out that higher dilution factor implies that large volume of water would be required, and for field implementation of LSWF, this can be costly. This problem can be handled with our model so that project cost and time are optimized. Using our developed model, only two laboratory experiments can be performed, and, through simulations, we can identify the optimum brine salinity required for an effective low salinity waterflooding process. By conducting one experiment with high salinity brine and another experiment using low salinity water, two relative permeability curves can be found by employing the model in this study (history matching process). Then, various simulation cases can be investigated using different dilutions of the high salinity brine. The optimum salinity for the injection brine can then be obtained.

We demonstrated this concept using the Yousef et al. [27] LSWF data sets. Yousef et al. [27] used seawater as the high salinity water and SW/100 as the low salinity water. However, the SW/100 did not produce any significant incremental oil recovery, hence, the SW/20 was used as the low salinity water for this study. After obtaining the history matched relative permeability curves for the two injection brines, several simulation cases were conducted, using different dilutions of the seawater (ranging from 2 to 15 times dilution). The oil recoveries of the new injected brines were compared with the oil produced by the SW/20 case. Fig. 16 shows the simulation outcome, and it can be observed that diluting the seawater increased the oil recovery. However, the difference between the oil recoveries becomes insignificant for dilutions beyond the SW/10, with the difference between the SW/20 and the SW/10 oil recoveries only about 2.6 % OOIP. The SW/15 and the SW/20 produced similar oil, suggesting that the optimum salinity for this reservoir system can be the SW/15. This simulation results indicate that the model can be used as a tool to estimate the optimum dilution of the high salinity brine.

4. Discussion

This section discusses the wettability alteration mechanism and the factors controlling it. The analysis is related to the WI values calculated at both the initial condition and the LSWF condition. It is noteworthy that the WI calculated values do not specifically give the wetting state of the reservoir (i.e., water-wet, oil-wet, or mixed-wet), however, they give an indication of the oil-brine-rock interactions dictating the wettability. Therefore, the WI calculated at initial condition can represent any of the wetting states, but it is expected that this initial WI is increased when low salinity brine is injected. Thus, an increase in the WI implies release of adsorbed oil from the mineral surface, shifting the initial wetting state towards a more water-wet condition, and this is consistent with the LSWF proposed mechanisms.

4.1. *Initial wettability and controlling factors*

Positive oil-brine interface ζ-potential values were calculated at the initial FW condition for all the simulated cores. It is worth pointing out that the oil-brine interface reactions are affected by both pH and brine composition. The equilibrium pH calculated at the initial conditions is in the range of 5.23 to 6.48, which is above the pH_{IEP} of crude oil.

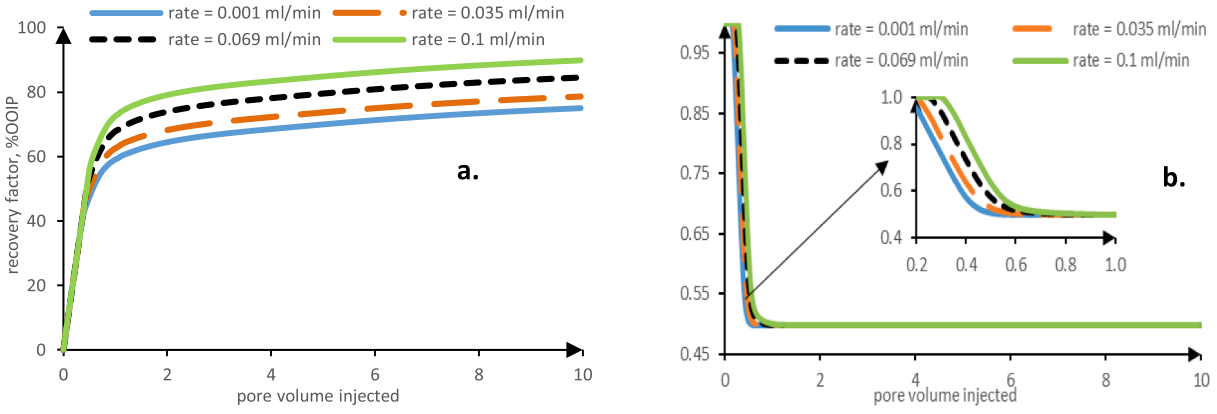

Fig. 15. Effect of injection rates on LSWF. (a) calculated oil recoveries at different injection rates, and (b) calculated total wettability indicator (β^{int}_{total}) at different injection rates.

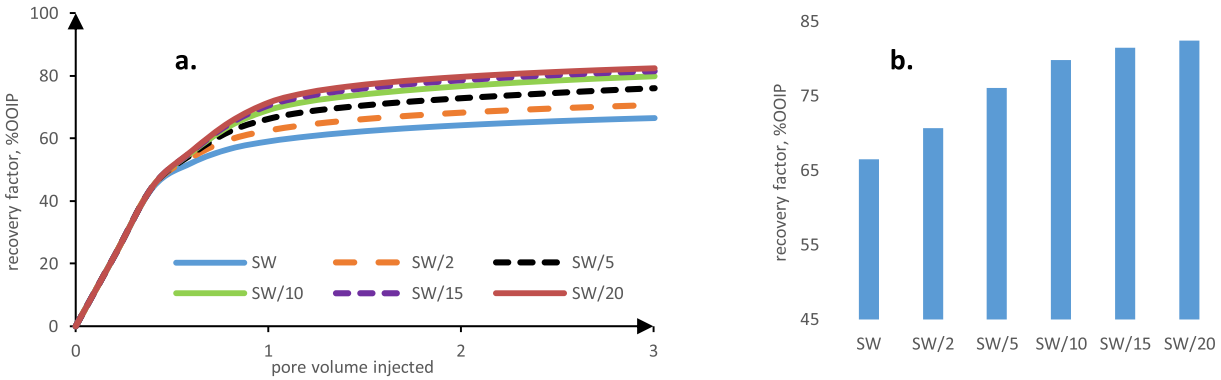

Fig. 16. (a) Calculated oil recoveries vs pore volumes injected, and (b) calculated ultimate oil recoveries for the various dilutions of the seawater.

Therefore, and one would expect the oil-brine interface to produce negative ζ-potentials. Similar results were observed by Jackson et al. [46] when they measured a positive oil-brine interface ζ-potential at carbonate reservoir condition (i.e., high pH condition). Besides, the proposed pH_{IEP} for crude oil (i.e., $pH_{IEP} < 5$) were measured in NaCl solutions at low ionic strengths, whereas the formation brines used for the simulations contain large amount of Ca^{+2} and Mg^{+2} ions, and the adsorption of these ions can make the ζ-potentials positive.

The same polarities of ζ-potentials were obtained for both the oil-brine and the rock-brine interfaces at the initial condition. However, smaller values of the WI were calculated at the initial condition compared to the WI values achieved at the low salinity injection condition. It should be noted that WI is the ratio of the concentration of free oil to the concentration of adsorbed oil. Therefore, decrease in the WI at the initial condition corresponds to the adsorption of oil at the mineral surface (i.e., small amount of free oil exists in the reservoir). Adsorption occurs between oppositively charged mineral-oil surface species, and Song et al. [108] proposed that oil can be adsorbed even when the crude oil and the mineral surfaces have the same polarities of ζ-potentials. This suggests that the water-film between the oil and the rock surface might not be very stable, and the oil could be attracted to the rock surface. In other words, the disjoining pressure might not be strong enough to overcome the adsorption force. Jackson et al. [46] stated that the water-film is partially stable at high ionic strength even when the oil-brine and rock-brine interfaces have same polarities of ζ-potential. Therefore, the oil surface species can react with the opposite rock surface species to render the wettability. The carboxylic oil component generating smaller WI values implies that it is more adsorbed on the carbonate surface. In a study conducted by Boampong et al. [75], they proposed that carbonate wettability is controlled by only the oil-brine and the rock-brine interface ζ-potentials, and oil can be adsorbed only when the ζ-potentials are of opposite polarities.

However, results of the current study highlight that inclusion of other mechanisms in the WI could provide a more realistic situation where oil adsorption is possible when the ζ-potentials are of the same polarities. Nonetheless, results of the current study agree with Boampong et al's [75] findings, which state that the carbonate rock will be strongly oil wet only when magnitude of the ζ-potentials are significant (opposite oil-brine and rock-brine ζ-potentials).

4.2. Dilution effects on wettability alteration

The simulation results of this study showed that injection of the low salinity brines shifted both the oil-brine and rock-brine interface ζ-potentials to more negative values, consistent with literature [12,15,86,109–111]. Mahani et al. [12,111] indicated that dilution of brines decreases the ionic strength, which results in the expansion of the electrical double layer (EDL). The ζ-potential of the surface is thus reduced. Moreover, concentration of the potential determining ions (eg: Ca^{+2}, and Mg^{+2}) were reduced through dilution, and this resulted in the negative ζ-potentials. In other words, dissolution of brine decreased the concentration of positive surface species (i.e., $>CO_3Ca^{+}$, $>CO_3Mg^{+}$). Another contributing factor to the negative ζ-potentials is the high pH of the brines. High pH reduces the number of aqueous Ca^{+2} ions while the number of CO_3^{-2} ions are increased [112]. As a result, more carbonate ions could be adsorbed at the mineral surface, generating negatively charged ζ-potential at the rock surface [112]. Similarly, dissociation of the carboxylic oil component increases at high pH, decreasing the oil-brine interface ζ-potential.

Obtaining the same polarities of ζ-potentials would stabilise the water film, shifting the wettability to a more water-wet system. Takeya et al. [86] suggested that the large repulsive force generated from the oil-brine and the rock-brine interfaces can enhance the detachment of oil from the carbonate rock surface. Our calculated WI agrees with the above proposed mechanisms. This means the injection of low salinity water increased the carboxylic oil related WI values, signifying desorption of the acidic oil components from the mineral surface. This increased the oil recovery.

4.3. Brine composition effects on wettability alteration

The composition of the injection brine can also impact the performance of LSWF and oil recovery. It should be noted that the FW used in Austad et al. [36] experiment was devoid of SO_4^{-2} ion, whiles the low salinity water (the seawater and the seawater depleted of NaCl) contained SO_4^{-2} ion. Several investigators (Austad et al. [23–26,30]; Saw & Mandal [38]; Zekri et al. [33]; Zhang et al. [29]) have indicated that during the injection of low salinity water, SO_4^{2-} is adsorbed onto the mineral surface. The adsorbed SO_4^{2-} ion co-adsorbs Ca^{2+} and Mg^{2+} ions, which react and release the adsorbed carboxylic groups from the mineral surface. Beside the SO_4^{2-} effects, the low salinity brines used by Austad et al. [36] have low ionic strengths, and as we have previous mentioned, decreasing ionic strength shifts the oil-brine and rock-brine ζ-potentials towards negative values. Consequently, repulsion between the interfaces stabilises the water-film between the oil and the rock surface.

Regarding the seawater depleted of NaCl, the incremental oil recovery can further be attributed to the removal of NaCl from the brine. NaCl in the brine surrounds the carbonate surface, reducing the amount of the potential determining ions that reach the mineral surface. Therefore, eliminating NaCl makes the carbonate surface more readily available to the potential determining ions. The surface charge can be altered by the potential determining ions to influence the wettability alteration [25,36,39,68]. Na^{+} ion can also form Na-naphthenates at the calcite surface, and this can make the oil molecule more sticker to the mineral surface [28,113] (i.e., more oil-wet). Therefore, removing NaCl from the brine improved the oil recovery as the reservoir becomes less oil-wet. In other words, the reservoir is shifted to a more water-wet state

when NaCl is removed from the brine. Our simulation results showed a substantial increase in the carboxylic group-related WI values. This implies that much of the adsorbed carboxylic component is desorbed from the rock surface, increasing the oil recovery.

4.4. Rock quality effects on oil recovery

The simulation outcomes related to the Chandrasekhar & Mohanty [67] experimental data showed that the calculated WI for the SW/50 brine exceeded the WI values of the SW/20 brine. It was expected that the injection of the SW/50 at tertiary stage would recover more incremental oil than the SW/20 injection. However, Chandrasekhar & Mohanty [67] produced more additional oil at tertiary stage with the SW/20 brine compared with the SW/50 brine. Interestingly, in a separate secondary LSWF experiments conducted with the SW/20 and SW/50 brines, the SW/50 brine produced more oil (85 % OOIP) than the SW/20 brine (65 % OOIP). We propose that this discrepancy was caused by the petrophysical properties of the rock used to perform the two experiments. The two carbonate cores used for the study are obtained from the same formation, but from different wells. The cores, thus, have different porosities and permeabilities. The core used in conducting the tertiary SW/50 injection (denoted here as core A) has porosity and permeability values of 0.154 and 10 md, respectively. The core used for the tertiary SW/20 injection (referred to as core B) has porosity and permeability values of 0.136 and 17 md, respectively. For the secondary LSWF studies, core A was used for the SW/20 injection, and core B used for the SW/50 injection.

Following Mokhtari et al. [114], the effect of porosity and permeability on LSWF was investigated by using the concept proposed by Amaefule et al. [115] and Abbaszadeh et al. [116]. Based on the Kozeny-Carmen equation, Amaefule et al. [115] and Abbaszadeh et al. [116] developed the concept of flow zone indicator (FZI) and reservoir quality index (RQI) to characterise hydraulic flow units, Equation (30) – (32):

$$FZI = \frac{RQI}{\varphi_z} \tag{30}$$

$$RQI = 0.0314\sqrt{\frac{K}{\varphi_e}} \tag{31}$$

$$\varphi_z = \frac{1-\varphi_e}{\varphi_e} \tag{32}$$

where K is permeability in mD, φ_e is porosity and φ_z, normalised porosity index, is the ratio of grain volume to pore volume of the rock. Amaefule et al. [115] indicated that layers of similar FZI will exhibit similar fluid-flow characteristics within the reservoir. It should be noted that Mokhtari et al. [114] observed linear relationship between flow zone indicator and LSWF oil recovery factor in carbonate rocks. Specifically, high recovery was attained as the flow zone indicator increased. Mokhtari et al. [114] suggested that rock quality affects LSWF oil recovery and that different recoveries can be achieved at different layers of the reservoir. However, they did not highlight how FZI impacted the observed oil recovery trend. Fig. 17 depicts our calculated flow zone indicator values for the two carbonate cores used by Chandrasekhar & Mohnaty [67]. A linear trend is obtained between the oil recoveries and the calculated FZI values, consistent with Mokhtari et al. [114] results.

It can be observed that core B, having higher flow zone indicator, produced more oil than core A at both secondary and tertiary stages of the oil recoveries. It should be noted that regarding the tertiary oil recoveries, FW injection at secondary stage recovered 40 % of OOIP in both core A and B. Therefore, the effect of water saturation on the performance of SW/20 and SW/50 at tertiary stage is ignored. This shows that oil recovery by LSWF in carbonate rocks is not only controlled by the carbonate-oil-brine interactions, but also permeability and porosity of the rock.

To further investigate the relationships between FZI, WI and oil recovery, we calculated the WI and FZI for Yousef et al. [27] experimental results. Yousef et al. [27] conducted two experiments (first flood and second flood) under the same experimental conditions. However, the second flood recovered more oil than the first flood. It is noteworthy that the cores used by Yousef et al. [27] to perform the two experiments have different petrophysical properties and connate water saturation (S_{wc}). The composite core used for the first flood has average porosity, permeability, and S_{wc} of 0.251, 39.6 mD, 0.1044, respectively. On the other hand, the composite core used for the second flood has average porosity, permeability, and S_{wc} of 0.2465, 68.3 mD, 0.144, respectively. The model was used to simulate the first flood oil recoveries, and the result is presented in the results section of the study (Fig. 10). However, we qualitatively calculated the second flood WI and FZI, and compared them with the first flood values.

A higher flow zone indicator was obtained for the second flood compared with the first flood flow zone indicator (Fig. 18). This is consistent with the oil recoveries where the second flood recovered more oil than the first flood. Nonetheless, the first flood calculated WI (normalised WI) supersedes the second flood WI values (Fig. 19). Some investigators [117–119] have proposed that water saturation (S_{wc}) can positively influence LSWF oil recovery. This is because S_{wc} serves as a

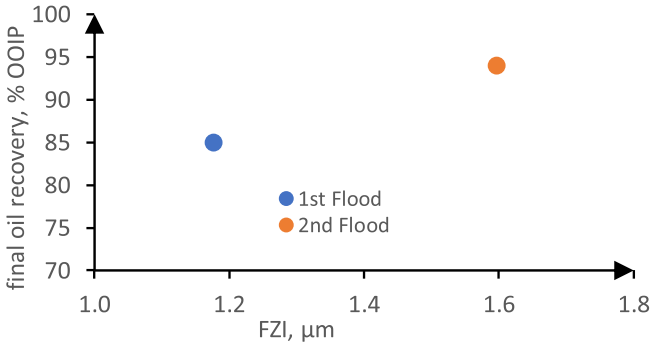

Fig. 18. Relationship between oil recoveries and flow zone indicator.

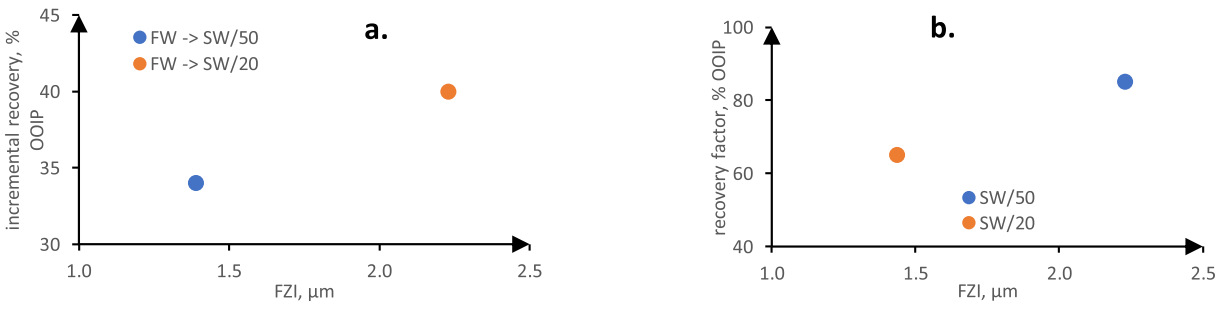

Fig. 17. Relationship between oil recoveries and flow zone indicator. (a) tertiary LSWF, and (b) secondary LSWF.

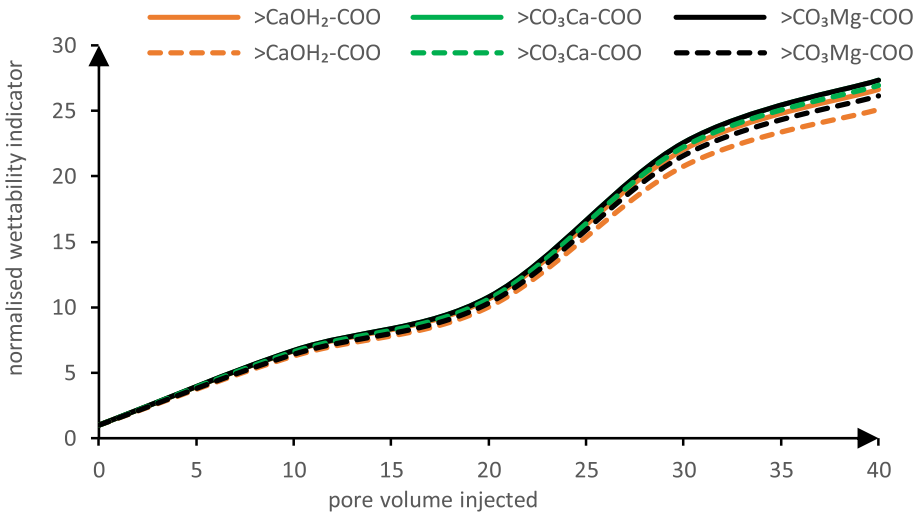

Fig. 19. Calculated WI (normalised) for the two core floods. Solid lines are for the first core flood WI results, and dash lines for the second core flood WI results.

conductive path, providing efficient interaction between the mineral surface and the injected brine [118]. Nevertheless, S_{wc} can have negative impact on the LSWF performance when it exceeds a certain limit [118]. The S_{wc} for the second flood was greater than the S_{wc} for the first flood. However, we do not consider S_{wc} to have contributed positively to the second core flood carbonate-oil-brine interactions based on the calculated WI values.

Mohammadkhani et al. [117] performed secondary LSWF experiments, and they observed that oil produced from the high permeability-high porosity carbonate rock (denoted as test 5) was higher than the oil recovered from the low permeability-low porosity rock (denoted as test 2). We calculated the FZI for this experiment, and similar trend was observed. That is, the oil recoveries increased with increased flow zone indicator (Fig. 20). Moreover, the calculated WI values of Test 5 were larger when compared to Test 2 WI values.

Our model confirms that a linear relationship exists between carbonate rock oil recovery and FZI, and that the oil recovery increased with increased FZI. It can be suggested that high FZI corresponds to a more conductive porous media, where fluid-flow through the rock is relatively ease. Therefore, cores generating high FZI will tend to produce more oil. Nonetheless, the study did not find direct relationship between FZI and WI in carbonate reservoirs. It was observed from our simulations corresponding to the Chandrasekhar & Mohanty [67] and Yousef et al. [27] experimental tests that WI is inversely proportional to FZI. However, our simulations relevant to Mohammadkhani et al. [117] experimental tests showed otherwise. Nevertheless, the study showed that FZI can substantially impact LSWF oil recovery. Therefore, porosity–permeability relation (i.e., rock quality) should be considered in planning LSWF projects.

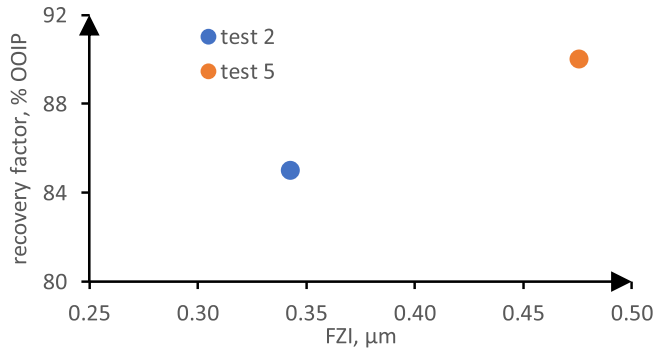

Fig. 20. Relationship between oil recoveries and flow zone indicator calculated for Mohammadkhani et al. [117] experimental results.

4.5. Effects of calcite dissolution on wettability alteration

The model results showed no occurrence of calcite dissolution for all the simulated experimental data. Previous investigators (Chandrasekhar & Mohanty [67], Yousef et al. [27], and Austad et al. [36]) observed mineral dissolution in their experiments which were largely credited to anhydrite dissolution. We are therefore of the view that the model is consistent with their observations. Moreover, the model calculated effluent ions are in good agreement with Chandrasekhar & Mohanty [67] results. It is worth mentioning that the degree of mineral dissolution is largely affected by the degree of undersaturation of the injection brine. The model result implies that the injected low salinity brines are either close to saturation or at saturation with the Ca^{+2} and CO_3^{-2} ions, hence, no calcite dissolution occurred. We therefore propose that calcite dissolution did not have an impact on the calculated WI values following the LSWF. Our results are in agreement with Mahani et al. [12] and Nasralla et al. [42] that dissolution may only enhance low salinity water effect as a secondary mechanism, and that calcite dissolution is not the main mechanism of LSWF in carbonate reservoirs.

4.6. Optimization of LSWF oil recovery

LSWF oil recovery involves physical and chemical displacements [104,120], and both processes can be influenced by the injection rate. It is worth noting that while physical displacement happens immediately when water is injected into the reservoir, chemical displacement requires some time. This is due to the time needed for the aqueous ions to react with the rock and the oil surfaces [120]. It should be noted that the chemical displacement process can desorb oil from the rock surface and alter the initial wettability of the reservoir. Lower injection rate ensured more contact time for the aqueous ions to interact with the rock and the oil surfaces. The 0.001 ml/min injection rate produced the highest total WI (at the early stages of the brine injections) as more interactions occurred between the aqueous ions and the carbonate-oil surfaces. Consequently, more oil was desorbed from the rock surface, shifting the wettability towards a more water-wet state. However, the 0.001 ml/min injection rate recovered the lowest amount of oil during the early stages of the brine injections. This implies that the oil recovery was not controlled by chemical displacement, but physical displacement. Therefore, increasing the injection rate increased the final oil recoveries, where the 0.1 ml/min injection rate produced the highest amount of oil. This suggests that to maximize LSWF oil recovery factor, high injection

rates can be considered. However, extreme rates can sometimes be detrimental as part of the reservoir can remained untouched by the injection brine [120]. Moreover, rate selection must be bounded by other factors such as pump capacity, bottom hole pressure, and fracturing criterial of the reservoir.

The simulation results also showed that a higher oil recovery could be achieved from the secondary injection of low salinity water compared to the tertiary injection of low salinity water. Shiran and Skauge [105] suggested that conducting tertiary LSWF can reduce the ultimate oil recovery. They indicated that the injection of high salinity brine at the secondary stage (before the start of low salinity waterflood) can cause effective trapping of oil clusters, and this reduces the ultimate oil recovery. On the other hand, an early injection of the low salinity water can ensure that continuous oil phase exists, and this increases the effective mobilisation of the oil. The oil recovery is then improved. The simulation outcomes of this study are consistent with the results reported by Egbe et al. [104], Shiran and Skauge [105], Rivet et al. [107], and Gamage and Thyne [121]. Based on the simulation results presented, we propose that, to optimise LSWF oil recovery in carbonate reservoirs, timing of the low salinity water injection and injection rate are essential parameters that can be considered.

5. Conclusions

This study was conducted to investigate the relationship between the carbonate-oil-brine geochemical interactions and the carbonate wettability. A new wettability alteration model which integrates three suggested LSWF mechanisms (surface charge alteration/ζ-potentials, ion exchange, and calcite dissolution) was developed. Findings from the simulations performed with this model can improve our understanding of the LSWF process. The proposed model produced results that are consistent with experimental LSWF data sets, suggesting that the model can be applied to evaluate LSWF projects and make an informed decision.

The outcomes of the study showed that adsorption of oil component on the carbonate rock surface is still possible even when the oil-brine and the rock-brine interfaces have the same polarities of ζ-potentials. Therefore, the wettability alteration is not related to only the polarities of the oil-brine and the rock-brine interface ζ-potentials produced from the carbonate-oil-brine interactions, but also, magnitude of the ζ-potentials. It was also demonstrated that lower injection rates improved the wettability alteration of the carbonate reservoirs (to a more water-wet state); however, this occurred at the early stages of the brine injection, without contributing to the oil recovery. Therefore, we conclude that physical displacement dominated the oil recovery process over chemical displacement. Consequently, the 0.1 ml/min injection rate recovered 90 % OOIP while the 0.001 ml/min injection rate produced 75 % OOIP. The results further indicated that tertiary injection of the low salinity water (compared to secondary injection) decreased the oil recovery by about 4 % OOIP. Finally, it was observed that LSWF oil recovery is not only controlled by the wettability alteration, but also by the quality of the carbonate rock. Therefore, we propose that the porosity–permeability relation (i.e., rock quality) should be considered in planning LSWF projects.

CRediT authorship contribution statement

Lawrence Opoku Boampong: Conceptualization, Data curation, Writing – review & editing, Writing – original draft. **Roozbeh Rafati:** Conceptualization, Supervision, Writing – review & editing. **Amin Sharifi Haddad:** Conceptualization, Supervision, Writing – review & editing.

Declaration of Competing Interest

The authors declare that they have no known competing financial interests or personal relationships that could have appeared to influence the work reported in this paper.

Data availability

Data will be made available on request.

Acknowledgments

Authors would like to thank the School of Engineering at the University of Aberdeen for providing required consumables and facilities to complete this research. We also thank Ghana Education Trust Fund (GETfund) for their financial support.

Appendix A:. Calculating the amount of mineral α initially present in the rock

The number of moles of mineral α initially present in the rock is calculated as follows:

Given the rock density, $\rho\ \left(\frac{kg}{L}\right)$, and porosity ($\varphi$), the grain mass, m (kg) is expressed as:

$$m = \rho V_g \tag{33}$$

where the grain volume, $V_g\ (L)$ is given as:

$$V_g = (1-\varphi)V_b \tag{34}$$

Given the % amount of mineral α present in the rock (eg: 10 % dolomite present in the carbonate rock, $f_\alpha = 0.1$), then, mass of mineral α present in the rock, m_α (kg) is:

$$m_\alpha = mf_\alpha = \rho V_g f_\alpha \tag{35}$$

$$m_\alpha = \rho(1-\varphi)V_b f_\alpha \tag{36}$$

Therefore, amount of mineral α per unit volume of water present in the gridblock is calculated as:

$$n_\alpha^0 = \frac{m_\alpha}{M_\alpha \times V_{H_2O}} = \frac{\rho(1-\varphi)V_b f_\alpha}{M_\alpha \times V_{H_2O}} \tag{37}$$

$$V_{H_2O} = \varphi S_w V_b \tag{38}$$

$$n_\alpha^0 = \frac{\rho(1-\varphi)V_b f_\alpha}{M_\alpha \varphi S_w V_b} \tag{39}$$

$$n_{\alpha}^{0} = \frac{\rho(1-\varphi)f_{\alpha}}{M_{\alpha}\varphi S_{w}} \tag{40}$$

where f_{α} is mass fraction of mineral α present in the rock, V_{H_2O} denotes volume of water in the gridblock (L), and V_b is gridblock bulk volume (L). M_{α} is molecular weight of mineral $\alpha\left(\frac{kg}{mol}\right)$, S_w is water saturation n_{α}^{0} is amount of mineral α per unit volume of water in the gridblock $\left(\frac{mol}{L}\right)$.

References

[1] Buckley JS, Takamura K, Morrow NR. Influence of Electrical Surface Charges on the Wetting Properties of Crude Oils. SPE Res Eng 1989;4(03):332–40.
[2] Awolayo AN, Sarma HK, Nghiem LX, Group CM. A Comprehensive Geochemical-Based Approach at Modeling and Interpreting Brine Dilution in Carbonate Reservoirs. SPE Reserv Simul Conf 2017;27. https://doi.org/10.2118/182626-MS.
[3] Hirasaki GJ. Wettability: Fundamentals and Surface Forces. SPE Form Eval 1991;6:217–26.
[4] Awolayo AN, Sarma HK, Nghiem LX. Modeling the characteristic thermodynamic interplay between potential determining ions during brine-dependent recovery process in carbonate rocks. Fuel 2018;224:701–17.
[5] Buckley JS, Liu Y. Some mechanisms of crude oil/brine/solid interactions. J Pet Sci Eng 1998;20:155–60.
[6] Qiao C, Johns R, Li L. Understanding the Chemical Mechanisms for Low Salinity Waterflooding. SPE Eur Featur 78th EAGE Conf Exhib 2016. https://doi.org/10.2118/180138-MS.
[7] Buckley, J. S. Evaluation of Rservoir Wettability and its Effect on Oil Recovery. *Report* (1997).
[8] Brady PV, Thyne G. Functional Wettability in Carbonate Reservoirs. Energy Fuels 2016;30(11):9217–25.
[9] Hiorth A, Cathles LM, Madland MV. The Impact of Pore Water Chemistry on Carbonate Surface Charge and Oil Wettability. Transp Porous Media 2010;85(1):1–21.
[10] Hiorth, A., Cathles, L. & Madland, M. V. Chemical modelling of wettability change in carbonate rocks Effect of Wettability on the Mechanical Stability of Chalk View project. (2008).
[11] Puntervold T, Mamonov A, Piñerez Torrijos ID, Strand S. Adsorption of Crude Oil Components onto Carbonate and Sandstone Outcrop Rocks and Its Effect on Wettability. Energy Fuels 2021;35(7):5738–47.
[12] Mahani H, Keya AL, Berg S, Bartels W-B, Nasralla R, Rossen WR. Insights into the mechanism of wettability alteration by low-salinity flooding (LSF) in carbonates. Energy Fuels 2015;29(3):1352–67.
[13] Su W, et al. New insights into the mechanism of wettability alteration during low salinity water flooding in carbonate rocks. J Dispers Sci Technol 2019;40:695–706.
[14] Zhang P, Austad T. The relative effects of acid number and temperature on chalk wettability. Proc - SPE Int Symp Oilf Chem 2005;185–191. https://doi.org/10.2118/92999-ms.
[15] Yousef AA, Al-Saleh S, Al-Jawfi M. Improved/enhanced oil recovery from carbonate reservoirs by tuning injection water salinity and ionic content. Proc - SPE Symp Improv Oil Recover 2012;1:819–36.
[16] Zaheri SH, Khalili H, Sharifi M. Experimental investigation of water composition and salinity effect on the oil recovery in carbonate reservoirs. Oil Gas Sci Technol 2020;75:21.
[17] Shariatpanahi SF, Strand S, Austad T. Initial wetting properties of carbonate oil reservoirs: Effect of the temperature and presence of sulfate in formation water. Energy Fuels 2011;25(7):3021–8.
[18] Martin J. The Effects of Clay on the Displacement of Heavy Oil by Water. *3rd Annu.* Meet Soc Pet Eng AIME 1959:1–24. https://doi.org/10.2118/1411-G.
[19] Tang GQ, Morrow NR. Influence of brine composition and fines migration on crude oil/brine/rock interactions and oil recovery. J Pet Sci Eng 1999;24:99–111.
[20] Xina X, Morrow NR. Wetting of quartz by oleic/aqueous liquids and adsorption from crude oil. Colloids Surfaces A Physicochem Eng Asp 1998;138:97–108.
[21] Jadhunandan PP, Morrow NR. Effect of Wettability on Waterflood Recovery for Crude-Oil/Brine/Rock Systems. SPE Reserv Eng 1995;10:40–6.
[22] Tang GQ, Morrow NR. Salinity, Temperature, Oil Composition, and Oil Recovery by Waterflooding. SPE Reserv Eng 1997;12:269–76.
[23] Zhang P, Austad T. Wettability and oil recovery from carbonates: Effects of temperature and potential determining ions. Colloids Surfaces A Physicochem Eng Asp 2006;279:179–87.
[24] Puntervold T, Strand S, Austad T. Water flooding of carbonate reservoirs: Effects of a model base and natural crude oil bases on chalk wettability. Energy Fuels 2007;21:1606–16.
[25] Fathi SJ, Austad T, Strand S. 'smart water' as a wettability modifier in chalk: The effect of salinity and ionic composition. Energy Fuels 2010;24(4):2514–9.
[26] Austad T, Shariatpanahi SF, Strand S, Black CJJ, Webb KJ. Conditions for a low-salinity Enhanced Oil Recovery (EOR) effect in carbonate oil reservoirs. Energy Fuels 2012;26(1):569–75.
[27] Yousef AA, Al-Saleh S, Al-Kaabi A, Al-Jawfi M. Laboratory investigation of novel oil recovery method for carbonate reservoirs. Soc Pet Eng - Can Unconv Resour Int Pet Conf 2010;2010(3):1825–59.
[28] Prabhakar S, Melnik R. Wettability alteration of calcite oil wells: Influence of smart water ions. Sci Rep 2017;7:2–10.
[29] Lager, A., Webb, K. J., Black, C. J. J., Singleton, M. & Sorbie, K. S. Low Salinity Oil Recovery - An Experimental Investigation. 0–12 (2008) doi:SPWLA-2008-v49n1a2.
[30] RezaeiDoust A, Puntervold T, Austad T. Chemical verification of the EOR mechanism by using low saline/smart water in sandstone. Energy Fuels 2011;25(5):2151–62.
[31] Zhang P, Tweheyo MT, Austad T. Wettability alteration and improved oil recovery in chalk: The effect of calcium in the presence of sulfate. Energy Fuels 2006;20:2056–62.
[32] Gupta R, et al. Enhanced waterflood for Middle East carbonate cores - Impact of injection water composition. *SPE Middle East Oil Gas Show Conf. MEOS*. Proc 2011;3:2052–72.
[33] Zekri, A., Khalifi, M. J. & Al-attar, H. Modification of Gulf Seawater for Possible Use in Improving Oil Recovery of Carbonate Formation : Mechanism Investigation. **29**, 12960–12976 (2020).
[34] Seyyedi M, Tagliaferri S, Abatzis J, Nielsen SM. An integrated experimental approach to quantify the oil recovery potential of seawater and low-salinity seawater injection in North Sea chalk oil reservoirs. Fuel 2018;232:267–78.
[35] Hiorth A, Evje S. A mathematical model for dynamic wettability alteration controlled by water-rock chemistry. Networks Heterog Media 2010;5:217–56.
[36] Austad T, Shariatpanahi SF, Strand S, Aksulu H, Puntervold T. Low Salinity EOR Effects in Limestone Reservoir Cores Containing Anhydrite: A Discussion of the Chemical Mechanism. Energy Fuels 2015;29(11):6903–11.
[37] Romanuka J, et al. Low Salinity EOR in Carbonates. SPE Improv Oil Recover Symp 2012. https://doi.org/10.2118/153869-MS.
[38] Saw RK, Mandal A. A mechanistic investigation of low salinity water flooding coupled with ion tuning for enhanced oil recovery. RSC Adv 2020;10:42570–83.
[39] Saeedi Dehaghani AH, Ghalamizade Elyaderani SM. Application of ion-engineered Persian Gulf seawater in EOR: effects of different ions on interfacial tension, contact angle, zeta potential, and oil recovery. Pet Sci 2021;18:895–908.
[40] Zahid A, Shapiro A, Stenby EH. Smart Waterflooding in Carbonate Reservoirs. J Pet Technol 2011;2800–2800.
[41] Omekeh AV, Friis HA, Fjelde I, Evje S. Modeling of Ion-Exchange and Solubility in Low Salinity Water Flooding. SPE Improv Oil Recover Symp 2012. https://doi.org/10.2118/154144-MS.
[42] Nasralla, R. A. *et al.* Demonstrating the potential of low-salinity waterflood to improve oil recovery in carbonate reservoirs by qualitative coreflood. *Soc. Pet. Eng. - 30th Abu Dhabi Int. Pet. Exhib. Conf. ADIPEC 2014 Challenges Oppor. Next 30 Years* **5**, 3476–3493 (2014).
[43] Li S, Jackson MD, Agenet N. Role of the calcite-water interface in wettability alteration during low salinity waterflooding. Fuel 2020;276:118097.
[44] Abdallah W, et al. Fundamentals of Wettability. Oilf Rev 2007;44–61. https://doi.org/10.6028/NBS.IR.78-1463.
[45] Sari A, Xie Q, Chen Y, Saeedi A, Pooryousefy E. Drivers of Low Salinity Effect in Carbonate Reservoirs. Energy Fuels 2017;31(9):8951–8.
[46] Jackson MD, Al-Mahrouqi D, Vinogradov J. Zeta potential in oil-water-carbonate systems and its impact on oil recovery during controlled salinity water-flooding. Sci Rep 2016;6:1–13.
[47] McGuire PL, Chatham JR, Paskvan FK, Sommer DM, Carini FH. Low Salinity Oil Recovery: An Exciting New EOR Opportunity for Alaska's North Slope. SPE West Reg Meet 2005;1–15. https://doi.org/10.2118/93903-MS.
[48] Hao J, Mohammadkhani S, Shahverdi H, Esfahany MN, Shapiro A. Mechanisms of smart waterflooding in carbonate oil reservoirs - A review. J Pet Sci Eng 2019;179:276–91.
[49] Soumitra B, Nande SDP. A review on low salinity waterflooding in carbonates: challenges and future perspective. J. Pet. Explor. Prod. Technol. 2021.
[50] Jerauld GR, Lin CY, Webb KJ, Seccombe JC. Modeling Low-Salinity Waterflooding. Modeling Low-Salinity Waterflooding 2008;11(06):1000–12.
[51] Kazemi, A., Korrani, N., Fu, W., Sanaei, A. & Sepehrnoori, K. Mechanistic Modeling of Modified Salinity Waterflooding in Carbonate. (2015).
[52] R, K. & J, K. Studying the Potential of Calcite Dissolution on Oil Liberation from Rock Surfaces during Single-Well-Chemical-Tracer Tests by Coupling a Multiphase Flow Simulator to the Geochemical Package. *J. Pet. Environ. Biotechnol.* **09**, 1–9 (2018).
[53] Dang, C. T. Q., Nghiem, L. X., Modeling, C. & Chen, Z. Modeling Low Salinity Waterflooding : Ion Exchange , Geochemistry and Wettability Alteration. (2013).
[54] Adedepa N. Awolayo, H. K. S. and L. X. N. A Comprehensive Geochemical-Based Approach at Modeling and Interpreting Brine Dilution in Carbonate Reservoirs. *SPE* 27 (2017).
[55] Brady PV, Krumhansl JL, Mariner PE. Surface complexation modeling for improved oil recovery. Proc - SPE Symp Improv Oil Recover 2012;1:376–85.
[56] Ghorbani M, Fariborz Rashidi A-M-D. Investigation of crude oil properties impact on wettability alteration during low salinity water flooding using an improved geochemical model. Sci Rep 2022;14.
[57] Qiao C, Johns R, Li L. Modeling Low-Salinity Waterflooding in Chalk and Limestone Reservoirs. Energy Fuels 2016;30:884–95.

[58] Himanshu Sharma KKM. Modeling of low salinity waterflooding in carbonates: Effect of rock wettability and organic acid distribution. J Pet Sci Eng 2021;16.
[59] Korrani AKN, Jerauld GR, Sepehrnoori K. Mechanistic modeling of low-salinity waterflooding through coupling a geochemical package with a compositional reservoir simulator. SPE Reserv Eval Eng 2016;19:142–62.
[60] Zivar D, Ishanov A, Pourafshary P. Insights into wettability alteration during low-salinity water flooding by capacitance-resistance model. Pet Res 2022. https://doi.org/10.1016/j.ptlrs.2022.01.004.
[61] Nguyen N, Dang C, Gorucu SE, Nghiem L, Chen Z. The role of fines transport in low salinity waterflooding and hybrid recovery processes. Fuel 2020;263.
[62] Alshakhs MJ, Kovscek AR. Understanding the role of brine ionic composition on oil recovery by assessment of wettability from colloidal forces. Adv Colloid Interface Sci 2016;233:126–38.
[63] Tetteh, J. T., Barimah, R. & Korsah, P. K. Ionic Interactions at the Crude Oil – Brine – Rock Interfaces Using Di ff erent Surface Complexation Models and DLVO Theory : Application to Carbonate Wettability. (2022).
[64] Xie Q, et al. The low salinity effect at high temperatures. Fuel 2017;200:419–26.
[65] Taheriotaghsara M, Bonto M, Nick HM, Eftekhari AA. Estimation of calcite wettability using surface forces. J Ind Eng Chem 2021;98:444–57.
[66] Yousef AA, Al-Saleh SH, Al-Kaabi A, Al-Jawfi MS. Laboratory Investigation of the Impact of Injection-Water Salinity and Ionic Content on Oil Recovery From Carbonate Reservoirs. SPE Reserv Eval Eng 2011;14:578–93.
[67] Chandrasekhar S, Mohanty KK. Wettability alteration with brine composition in high temperature carbonate reservoirs. Proc - SPE Annu Tech Conf Exhib 2013;3:2416–32.
[68] Fathi SJ, Austad T, Strand S. Water-based enhanced oil recovery (EOR) by 'smart water': Optimal ionic composition for EOR in carbonates. Energy Fuels 2011;25:5173–9.
[69] Ravat C, Dumonceau J, Monteil-Rivera F. Acid/base and Cu(II) binding properties of natural organic matter extracted from wheat bran: Modeling by the surface complexation model. Water Res 2000;34:1327–39.
[70] Sø HU, Postma D, Jakobsen R, Larsen F. Competitive adsorption of arsenate and phosphate onto calcite; experimental results and modeling with CCM and CD-MUSIC. Geochim Cosmochim Acta 2012;93:1–13.
[71] Bonto, M., Eftekhari, A. A. & Nick, H. A calibrated model for the carbonate-brine-crude oil surface chemistry and its effect on the rock wettability, dissolution, and mechanical properties. *Soc. Pet. Eng. - SPE Reserv. Simul. Conf. 2019, RSC 2019* (2019) doi:10.2118/193865-ms.
[72] Korrani AKN, Jerauld GR. Modeling wettability change in sandstones and carbonates using a surface-complexation-based method. J Pet Sci Eng 2019;174:1093–112.
[73] Bonto M, Eftekhari AA, Nick M, H.. Wettability Indicator Parameter Based on the Thermodynamic Modeling of Chalk-Oil-Brine Systems. Energy Fuels 2020;34:8018–36.
[74] Takeda M, Manaka M, Tuji T. Chemical osmosis as a cause for the improved oil recovery by low-salinity water flooding: Experimental and numerical approaches for detection. J Pet Sci Eng 2021;207:109090.
[75] Boampong LO, Rafati R, Sharifi Haddad A. A calibrated surface complexation model for carbonate-oil-brine interactions coupled with reservoir simulation - Application to controlled salinity water flooding. J Pet Sci Eng 2022;208:109314.
[76] Delshad M, Pope GA, Sepehrnoori K. A compositional simulator for modeling surfactant enhanced aquifer remediation, 1 Formulation. J Contam Hydrol 1996;23:303–27.
[77] Parkhurst, B. D. L. User ' s Guide to PHREEQC — a Computer Program for Inverse Geochemical Calculations. (1995).
[78] Parkhurst DL, Wissmeier L. PhreeqcRM: A reaction module for transport simulators based on the geochemical model PHREEQC. Adv Water Resour 2015;83:176–89.
[79] Eftekhari AA, Thomsen K, Stenby EH, Nick HM. Thermodynamic Analysis of Chalk-Brine-Oil Interactions. Energy Fuels 2017;31:11773–82.
[80] Stipp SLS. Toward a conceptual model of the calcite surface: Hydration, hydrolysis, and surface potential. Geochim Cosmochim Acta 1999;63:3121–31.
[81] Heberling F, et al. Reactivity of the calcite-water-interface, from molecular scale processes to geochemical engineering. Appl Geochemistry 2014;45:158–90.
[82] Song, J. *et al.* Surface complexation modeling of calcite zeta potential in mixed brines for carbonate wettability characterization. *Eng. Sci. Fundam. 2017 - Core Program. Area 2017 AIChE Annu. Meet.* **2**, 947–954 (2017).
[83] Sø, H. U. Adsorption of arsenic and phosphate onto the surface of calcite as revealed by batch experiments and surface complexation modelling. (2011). doi:10.13140/2.1.1196.1603.
[84] Heberling F, et al. Structure and reactivity of the calcite-water interface. J Colloid Interface Sci 2011;354:843–57.
[85] Li S, et al. Influence of surface conductivity on the apparent zeta potential of calcite. J Colloid Interface Sci 2016;468:262–75.
[86] Takeya M, Shimokawara M, Elakneswaran Y, Nawa T, Takahashi S. Predicting the electrokinetic properties of the crude oil/brine interface for enhanced oil recovery in low salinity water flooding. Fuel 2019;235:822–31.
[87] Kazemi Nia Korrani, A., Sepehrnoori, K. & Delshad, M. A comprehensive geochemical-based approach to quantify the scale problems. *SPE - Eur. Form. Damage Conf. Proceedings, EFDC* **2**, 946–964 (2014).
[88] Nia Korrani AK, Sepehrnoori K, Delshad M. A novel mechanistic approach for modeling low salinity water injection. SPE Annu Tech Conf Proc 2013;7:3206–23.
[89] Kazemi Nia Korrani, A., Sepehrnoori, K. & Delshad, M. Coupling IPhreeqc with UTCHEM to model reactive flow and transport. *Comput. Geosci.* **82**, 152–169 (2015).
[90] Nghiem L, Sammon P, Grabenstetter J, Ohkuma H. Modeling CO2 storage in aquifers with a fully-coupled geochemical EOS compositional simulator. Proc - SPE Symp Improv Oil Recover 2004.
[91] Hommel J, Coltman E, Class H. Porosity-Permeability Relations for Evolving Pore Space: A Review with a Focus on (Bio-)geochemically Altered Porous Media. Transp Porous Media 2018;124:589–629.
[92] Xie M, et al. Implementation and evaluation of permeability-porosity and tortuosity-porosity relationships linked to mineral dissolution-precipitation. Comput Geosci 2015;19:655–71.
[93] Goldberg S. Modeling Selenite Adsorption Envelopes on Oxides, Clay Minerals, and Soils using the Triple Layer Model. Soil Sci Soc Am J 2013;77:64–71.
[94] Goldberg S, Chunming S, Forster HS. Sorption of Molybdenum on Oxides, Clay Minerals, and Soils: Mechanisms and Models. Adsorption of Metals by Geomedia. Woodhead Publishing Limited; 1998. 10.1016/b978-012384245-9/50020-7.
[95] Hou WG, Song SE. Intrinsic surface reaction equilibrium constants of structurally charged amphoteric hydrotalcite-like compounds. J Colloid Interface Sci 2004;269:381–7.
[96] Castro A, Bhattacharyya K, Eisenthal KB. Energetics of adsorption of neutral and charged molecules at the air/water interface by second harmonic generation: Hydrophobic and solvation effects. J Chem Phys 1991;95:1310–5.
[97] Appelo, C.A.J. & Postma, D. Geochemistry, Groundwater and Pollution, 2nd Edition (2005).
[98] Hiemstra T, Van Riemsdijk WH. A surface structural approach to ion adsorption: The charge distribution (CD) model. J Colloid Interface Sci 1996;179:488–508.
[99] Cabrera-Guzman D, Swartzbaugh JT, Weisman AW. The use of electrokinetics for hazardous waste site remediation. J Air Waste Manag Assoc 1990;40:1670–6.
[100] Oscarson, D.W. & Hume, H.B. Effects of the Solid:Liquid Ratio on the Sorption of Sr^{2+} and Cs^{+} on Bentonite (1998).
[101] Ding H, Mettu S, Rahman S. Probing the Effects of Ca2+, Mg2+, and SO42-on Calcite-Oil Interactions by 'soft Tip' Atomic Force Microscopy (AFM). Ind Eng Chem Res 2020;59:13069–78.
[102] Chandrasekhar S, Sharma H, Mohanty KK. Dependence of wettability on brine composition in high temperature carbonate rocks. Fuel 2018;225:573–87.
[103] Sharma H, Mohanty KK. An experimental and modeling study to investigate brine-rock interactions during low salinity water flooding in carbonates. J Pet Sci Eng 2018;165:1021–39.
[104] Egbe DIO, Jahanbani Ghahfarokhi A, Nait Amar M, Torsæter O. Application of Low-Salinity Waterflooding in Carbonate Cores: A Geochemical Modeling Study. Nat Resour Res 2021;30:519–42.
[105] Shaker Shiran B, Skauge A. Enhanced oil recovery (EOR) by combined low salinity water/polymer flooding. Energy Fuels 2013;27:1223–35.
[106] Fani, M., Al-Hadrami, H., Pourafshary, P., Vakili-Nezhaad, G. & Mosavat, N. Optimization of smart water flooding in carbonate reservoir. *Soc. Pet. Eng. - Abu Dhabi Int. Pet. Exhib. Conf. 2018, ADIPEC 2018* (2019) doi:10.2118/193014-ms.
[107] Scott M Rivet, Larry W Lake, G. A. P. A Coreflood Investigation of Low-Salinity Enhanced Oil Recovery. *Soc. Pet. Eng. Annu. Tech. Conf. Exhib. Florence, Italy, Sept. 2010* **SPE-134297**, 20 (2010).
[108] Song J, et al. Evaluating physicochemical properties of crude oil as indicators of low-salinity–induced wettability alteration in carbonate minerals. Sci Rep 2020;10:1–16.
[109] Lu Y, Najafabadi NF, Firoozabadi A. Effect of Temperature on Wettability of Oil/Brine/Rock Systems. Energy Fuels 2017;31:4989–95.
[110] Rahimi A, Honarvar B, Safari M. The role of salinity and aging time on carbonate reservoir in low salinity seawater and smart seawater flooding. J Pet Sci Eng 2020;187:106739.
[111] Mahani H, Keya AL, Berg S, Nasralla R. Electrokinetics of Carbonate/Brine Interface in Low-Salinity Waterflooding: Effect of Brine Salinity, Composition, Rock Type, and pH on ζ-Potential and a Surface-Complexation Model. SPE J 2017;22:053–68.
[112] Farhadi H, Fatemi M, Ayatollahi S. Experimental investigation on the dominating fluid-fluid and rock-fluid interactions during low salinity water flooding in water-wet and oil-wet calcites. J Pet Sci Eng 2021;204:108697.
[113] Prabhakar S, Melnik R. Influence of Mg2+, SO42− and Na+ ions of sea water in crude oil recovery: DFT and ab initio molecular dynamics simulations. Colloids Surfaces A Physicochem Eng Asp 2018;539:53–8.
[114] Mokhtari R, Anabaraonye BU, Afrough A, Mohammadkhani S, Feilberg KL. Experimental investigation of low salinity water-flooding in tight chalk oil reservoirs. J Pet Sci Eng 2022;208:109282.
[115] Amaefule, J. O., Altunbay, M., Tiab, D., Kersey, D. G. & Keelan, D. K. Enhanced reservoir description: using core and log data to identify hydraulic (flow) units and predict permeability in uncored intervals/ wells. *Proc. - SPE Annu. Tech. Conf. Exhib.* **Omega**, 205–220 (1993).
[116] Abbaszadeh M, Fujii H, Fujimoto F. Permeability prediction by hydraulic flow units - Theory and applications. SPE Form Eval 1996;11:263–71.
[117] Mohammadkhani S, Shahverdi H, Esfahany MN. Impact of salinity and connate water on low salinity water injection in secondary and tertiary stages for enhanced oil recovery in carbonate oil reservoirs. J Geophys Eng 2018;15:1242–54.
[118] Zaeri MR, Shahverdi H, Hashemi R, Mohammadi M. Impact of water saturation and cation concentrations on wettability alteration and oil recovery of carbonate rocks using low-salinity water. J Pet Explor Prod Technol 2019;9:1185–96.
[119] Shehata AM, Kumar HT, Nasr-El-Din HA. New insights on relative permeability and initial water saturation effects during low-salinity waterflooding for

sandstone reservoirs. Soc Pet Eng - SPE Trinidad Tobago Sect Energy Resour Conf 2016. https://doi.org/10.2118/180874-MS.

[120] F Srisuriyachai, S Panthuvichien, T Phomsuwansiri, W. K. Effects of Injection Rate of Low Salinity Brine on Oil Recovery Mechanisms and Relative Permeability. *Eur. Assoc. Geosci. Eng.* **2016**, p. **1**, (2016).

[121] Gamage P, Thyne G. Comparison of oil recovery by low salinity waterflooding in secondary and tertiary recovery modes. Proc - SPE Annu Tech Conf Exhib 2011;5:4291–302.